

IMPACT OF DIETARY SALT ON BLOOD VESSEL HEALTH AND THE ROLE OF EXERCISE AND IMMUNE SYSTEM ACTIVATION

2024 | DENZEL ENRIQUE ERNEST MARICAN

B.Sc. HONOURS THESIS – BIOLOGY



**IMPACT OF DIETARY SALT ON BLOOD VESSEL HEALTH AND THE ROLE OF
EXERCISE AND IMMUNE SYSTEM ACTIVATION**

by

DENZEL ENRIQUE ERNEST MARICAN

A THESIS SUBMITTED IN PARTIAL FULFILLMENT
OF THE REQUIREMENTS FOR THE DEGREE OF

BACHELOR OF SCIENCE (HONS.)

in the

DEPARTMENT OF BIOLOGICAL SCIENCES



THOMPSON RIVERS UNIVERSITY

This thesis has been accepted as conforming to the required standards by:
Mark Rakobowchuk (Ph.D.), Thesis Supervisor, Dept. Biological Sciences
Natasha Ramroop-Singh (Ph.D.), Secondary Supervisor, Dept. Biological Sciences
Gregory Anderson (Ph.D.), External Examiner, Dept. Biological Sciences

Dated this 20th day of June 2024, in Kamloops, British Columbia, Canada

© Denzel Enrique Ernest Marican 2024

ABSTRACT

A diet that is high in salt is known to increase the risk of stroke and cardiovascular disease, which are leading causes of mortality worldwide (WHO 2024). Additionally, endothelial dysfunction is a common predictor of cardiovascular disease and an indicator of vascular impairment. While acute exercise is known to cause transient endothelial dysfunction, the combined effects of high salt intake and exercise remain unclear. The activation of the immune system from exercise or alterations in immune functions after high salt intake may contribute to endothelial dysfunction. In this study, participants underwent standardized acute exercise bouts during periods of salt and placebo supplementation. Ultrasound measurements of the brachial and popliteal arteries were taken to assess flow mediated dilation responses, effectively measuring endothelial function before and after exercise, and before and after high salt intake. Blood samples were also collected to analyze any changes in immune cell populations. Results indicate that exercise induced local endothelial dysfunction in the popliteal artery, suggesting that locally produced reactive oxygen species and glycocalyx damage due to increased shear stress were more significant factors than immune system activation and sodium related dysfunction in reducing flow-mediated dilation responses. Additionally, no significant changes were observed in leukocyte populations before and after exercise or salt supplementation, likely due to insufficient exercise stimulus, high variation in a small sample size, or the greater importance of alterations in immune cell functions, such as increases in pro-inflammatory phenotypes, rather than absolute counts.

Thesis Supervisor: Associate Professor Mark Rakobowchuk

ACKNOWLEDGEMENTS

First, I would like to extend my heartfelt gratitude to Dr. Mark Rakobowchuk for his invaluable guidance, support, and mentorship throughout my work on this project. Over the past few years, I have learned more than I ever imagined possible under his teaching and direction. This work would not have been possible without his knowledge, expertise, and understanding. I will carry his values of professionalism and care with me in my future endeavours. I would also like to express my sincere thanks to Thane Martin, with whom I spent countless hours in the lab. Thane's cooperation and guidance were instrumental in the completion of this project, and I could not have asked for a better teammate. I would also like to thank Alivia Mercer for providing constant support and feedback throughout the project and writing process. I am greatly appreciative of the time and care you provided to help me succeed. My sincere appreciation goes to the TRU UREAP for funding my research journey. I am also deeply grateful to Kathy Baethke and Matthew Francis for their instrumental role in teaching me about all the equipment and helping me gain confidence in the lab. Additionally, I would like to thank Dr. Natasha Ramroop-Singh for serving as my secondary supervisor and Dr. Greg Anderson for being my external examiner.

TABLE OF CONTENTS

<i>ABSTRACT</i>	<i>ii</i>
<i>ACKNOWLEDGEMENTS</i>	<i>iii</i>
<i>LIST OF FIGURES</i>	<i>vii</i>
<i>LIST OF TABLES</i>	<i>x</i>
<i>INTRODUCTION</i>	<i>1</i>
Endothelial surface layer	1
ESL in mechanotransduction	4
eNOS/NO/cGMP vasodilatory pathway	5
ESL as a non-osmotic salt buffer	8
Salt-induced increases in oxidative stress impair endothelial function	9
Salt induces endothelial cell stiffening and glycocalyx damage	12
Exercise-induced ESL damage	14
Damage to the ESL may liberate stored Na⁺	15
Effects of salt and exercise on immune response	15
Neutrophils.....	16
Monocytes and macrophages	17
Natural killer cells.....	18
Exercise as an immune system adjuvant.....	19
Objectives	19
<i>METHODS</i>	<i>20</i>
Ethics	20
Participants	20
Determining exercise capacity	20
Ventilatory threshold 1	21
Ventilatory threshold 2	24

Experimental design	26
Flow-mediated dilation	27
Antibody titration	30
Blood storage and preparation for flow cytometry	31
Flow cytometry	33
Gating strategy	34
Statistics	36
<i>RESULTS</i>.....	36
Popliteal FMD	36
Brachial FMD.....	39
Changes in baseline artery diameters	40
Flow cytometry of blood leukocyte populations.....	41
Cardiovascular fitness variables.....	44
<i>DISCUSSION</i>.....	44
Local glycocalyx shedding exerts a greater influence on endothelial dysfunction than the effects of high salt intake	45
Inflammation response to exercise	49
Leukocytosis post-exercise	50
Neutrophils	51
Monocytes and macrophages.....	54
Natural killer cells.....	57
Limitations.....	60
Changes to baseline vessel diameter post-exercise.....	61
Exercise training inhibits pathways of salt-related dysfunction	62
Dietary contributions to antioxidative capacity	63

<i>CONCLUSIONS</i>	63
<i>LITERATURE CITED</i>	65
<i>APPENDICES</i>	78
Appendix 1	78
Statistical analysis	78
Abbreviations	87

LIST OF FIGURES

Figure 1. Visual representation of the endothelial glycocalyx (left) and its major components (right). Glycoproteins are seen attached to basal endothelial cells. GAG chains are seen branching off from anchor proteoglycans and soluble proteoglycans which are incorporated with hyaluronic acid (HA), endothelial cell superoxide dismutase (ec-SOD), and antithrombin-III (AT III). These components form the endothelial glycocalyx that functions as a barrier between blood plasma and the endothelium and exerts various roles in plasma and vessel wall homeostasis (Reitsma et al. 2007). 2

Figure 2. The chemical structures of the main repeating disaccharide units and glycosidic bonds in GAGs. GAGs shown include heparin/heparan sulfate, chondroitin sulfates, hyaluronic acid/hyaluronan, and keratan sulfates. Hyaluronic acid stands out as the only GAG devoid of sulfate groups. The chemical structures of keratan sulfates are not provided (Afosah and Al-Horani 2020). 3

Figure 3. Diagram of NO pathway from synthesis to relaxation. NO prompts VSMC relaxation by activating GPCRs, triggering PLC, leading to calcium release. Calcium and other cofactors activate eNOS, producing NO. NO binds to sGC in VSMC, generating cGMP, which activates PKG, promoting VSMC relaxation. Shear stress can also activate eNOS independently of GPCR (da Silva et al. 2021). 7

Figure 4. Diagram of coupled versus uncoupled eNOS showing that uncoupled eNOS can generate O_2^- , a highly toxic super radical. Uncoupled eNOS can subsequently contribute to the development of various CVDs (Tran et al. 2022). 10

Figure 5. Summary of the oxidative stress-related pathways that excess dietary salt can disrupt causing endothelial dysfunction. Elevated dietary Na^+ levels increase O_2^- production by activating NADPH oxidase and inhibiting SOD-1 and mitochondrial SOD (SOD-2). NO reacts readily with O_2^- , preventing its diffusion into vascular smooth muscle. Although not shown, the resulting $ONOO^-$ oxidizes BH_4 , which leads to uncoupling of eNOS, leading to further reductions in NO and increases in O_2^- (Patik et al. 2021). 12

Figure 6. Comparing a healthy and damaged ESL, where damage to the eGC allows infiltration of Na^+ into endothelial cells causing decreased NO-mediated dilation and endothelial cell stiffness. To the left, the healthy glycocalyx acts as a protective barrier between the plasma and the

endothelial cell, buffering positively charged Na^+ . Conversely, elevated plasma Na^+ levels on the right result in glycocalyx damage, allowing increased Na^+ access to ENaC on the endothelial surface, consequently raising intracellular Na^+ concentrations. In such instances, cellular stiffness increases, and the conversion of shear stress into NO release is diminished (Patik et al. 2021).. 13

Figure 7. $\dot{V}\text{CO}_2$ over $\dot{V}\text{O}_2$ graph to identify VT1 through intersection points of linear components. The intersection point of the two linear segments represents VT1. Each point is from breath-by-breath data collected during an incremental ramp exercise test using Quark CPET metabolic cart (COSMED, Italy)..... 22

Figure 8. RQ over time to validate VT1 found on the $\dot{V}\text{CO}_2/\dot{V}\text{O}_2$ graph. The red line represents the threshold RQ of 1.0. Once RQ begins increasing and is below 1.0, VT1 will have been reached. 23

Figure 9. General outline of the identification of the first and second ventilatory thresholds (VT1 and VT2) through cardiopulmonary exercise testing (CPET). This includes a focused examination of parameters such as $\dot{V}\text{O}_2$ versus $\dot{V}\text{CO}_2$, $\text{VE}/\dot{V}\text{CO}_2$, $\text{VE}/\dot{V}\text{O}_2$, VE, and PET_{O_2} and PET_{CO_2} panels. "Watt" symbolizes the rising resistance encountered in ramp incremental testing. Although not shown, RQ over time may also be used for the determination of VT1, when it begins rising signalling a shift from aerobic to anaerobic metabolism and achievement of VT1 (Anselmi et al. 2021). 25

Figure 10. The screenshot of the CaroLab vessel wall tracking software illustrates several key features. Red circles highlight: (A) the conversion factor, (B) vessel wall tracking guide points, (C) the ruler tool used to determine the conversion factor, and (D) the average heart rate in beats per minute over the testing period. 29

Figure 11. The stain index is the ratio of the separation between the positive population (red) and the negative population (blue), divided by two times the standard deviation of the negative population. MFI is the mean fluorescence intensity for positive and negative populations (Kalser 2023). 31

Figure 12. A 1 mL aliquot of whole blood was lysed with red blood cell lysis buffer (10:1 ratio) in a 15 mL centrifuge tube, followed by centrifugation at 300 g to pellet the peripheral blood mononuclear cells (PBMCs). The lysed RBC layer was discarded, and the remaining pellet was washed with 5 mL of fluorescence-activated cell sorting buffer (FACS). After resuspension and incubation with Fc receptor blocker, the sample was stained with designated antibodies to identify

leukocyte populations. Stained samples were incubated, resuspended, and analyzed using a flow cytometer (Cytoflex, Beckman Coulter)..... 33

Figure 13. The flow cytometry gating strategy involved enumerating NK cell (CD56⁺), neutrophil (CD66b⁺), and monocyte (CD14⁺) populations. The absence of negative populations for CD45⁺ resulted from the isolation of white blood cells during the blood preparation procedure. Gating for two peaks within the CD56⁺ population was due to the presence of CD56⁺ bright and dim subpopulations, representing distinct subsets of NK cells..... 35

Figure 14. Exercise effects on popliteal artery flow-mediated dilation (n=4). Post-exercise popliteal FMD was reduced by 2.6% (95% CI: 1.8 to 3.5%, p < 0.01), as determined by post hoc analysis of exercise condition. Results are averaged over the levels of condition and time (n=4). 37

Figure 15. Effects of salt and sugar on popliteal FMD % including standard error bars. Results are averaged over the levels of exercise. None displayed significance (p>0.05) (n=4). 38

Figure 16. Brachial FMD % before and after a high salt diet and pre- and post-exercise showed no significant differences (n=4). 39

Figure 17. Brachial artery FMD % before and after salt intake and sugar intake. Results are averaged over the levels of exercise (n=4). 40

LIST OF TABLES

Table 1. Surface markers and fluorophores for immune cells.	32
Table 2. Post Hoc comparison of pre- and post-exercise conditions found a significant mean difference (n=4).	36
Table 3. Post Hoc comparison of condition and time displaying no significant differences (p>0.05) (n=4).	37
Table 4. Mean percent dilation of the popliteal artery for, condition (salt or sugar), time (before or after), and exercise (pre- and post-exercise) measured through FMD (n=4).	38
Table 5. Mean percent dilation of the brachial artery for, condition (salt or sugar), time (before or after), and exercise (pre- and post-exercise) measured through FMD (n=4).	39
Table 6. Baseline artery diameters displayed in μm (n=4).	41
Table 7. Leukocyte cells/ μL for, condition (salt or sugar), time (before or after), and exercise (pre- and post-exercise) measured through flow cytometry (n=4).	42
Table 8. Neutrophil cells/ μL for, condition (salt or sugar), time (before or after), and exercise (pre- and post-exercise) measured through flow cytometry (n=4).	42
Table 9. Monocyte cells/ μL for, condition (salt or sugar), time (before or after), and exercise (pre- and post-exercise) measured through flow cytometry (n=4).	42
Table 10. NK cells/ μL for, condition (salt or sugar), time (before or after), and exercise (pre- and post-exercise) measured through flow cytometry (n=4).	43
Table 11. Neutrophil percent of the total leukocyte population for, condition (salt or sugar), time (before or after), and exercise (pre- and post-exercise) measured through flow cytometry (n=4).	43
Table 12. Monocyte percent of the total leukocyte population for, condition (salt or sugar), time (before or after), and exercise (pre- and post-exercise) measured through flow cytometry (n=4).	43
Table 13. NK cell percent of the total leukocyte population for, condition (salt or sugar), time (before or after), and exercise (pre- and post-exercise) measured through flow cytometry (n=4).	44
Table 14. Cardiovascular fitness variables (n=4).	44

INTRODUCTION

The World Health Organization (WHO) (2023) recommends that the daily limit of salt intake for adults should not exceed 2000 mg per day. On average, people consume over 4000 mg of sodium (Na^+) every day (WHO 2023). Na^+ is a key cation in the extracellular fluid of the body which contributes to the maintenance of plasma volume through osmotic effects, acid-base balance, transmission of nerve impulses and normal cell function. However, excess Na^+ consumption is linked to increased risk of cardiovascular disease (CVD), increased arterial blood pressure (BP) and according to a meta-analysis conducted by Wang et al. (2020), the risk of CVD increases by up to 6% with each additional gram of daily Na^+ consumed. In 2023, the leading cause of death in the United States was CVD, ahead of cancer (CDC, 2024). It is widely known that high blood pressure (hypertension) causes CVD, contributes to kidney disease, and increases stroke incidence (Strazzullo et al., 2009). In these diseases, the blood vessel wall, specifically the lining called the endothelium, is the first site of dysfunction that leads to structural damage of the arterial wall, atherosclerotic plaque formation, and potentially CVD (Widmer and Lerman, 2014).

Endothelial surface layer

The endothelium has a layer of complex sugar molecules on its surface called the endothelial surface layer (ESL). The glycocalyx is a key component of the ESL that is anchored by glycoproteins and proteoglycans, which form a system in which soluble molecules can further incorporate into its structure (Reitsma et al. 2007). Glycoproteins and proteoglycans are considered the “backbone” molecules of the glycocalyx (Figure 1). Glycoproteins connect the glycocalyx to the endothelial cell membrane and function as endothelial cell adhesion molecules that play a major role in cell recruitment from the bloodstream, and in cell signalling (Reitsma et al. 2007).

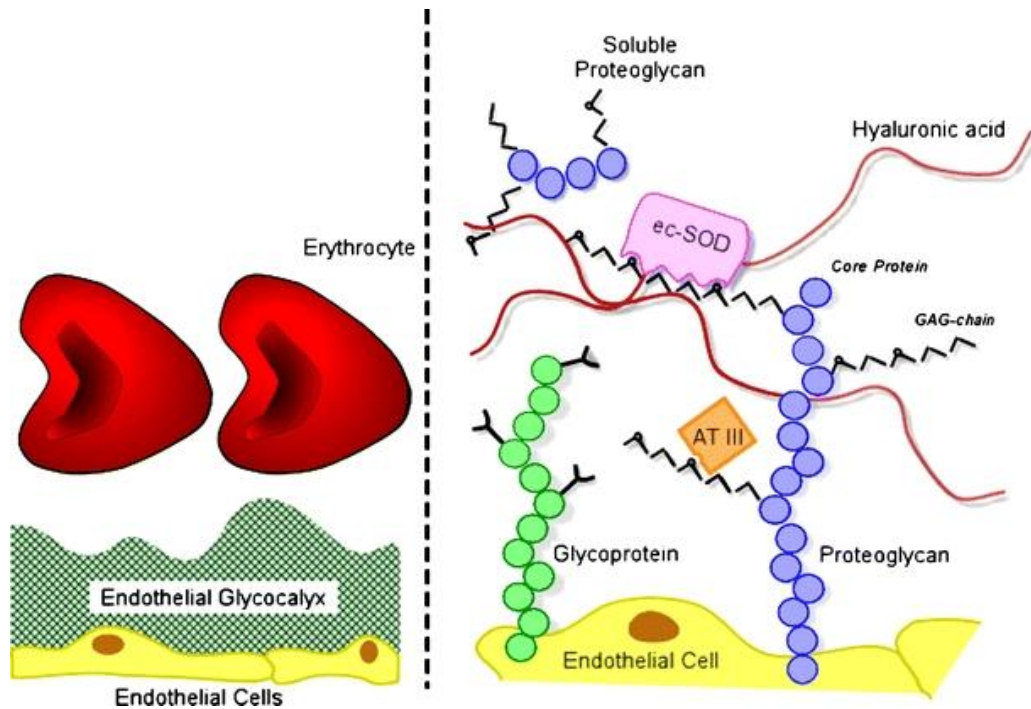


Figure 1. Visual representation of the endothelial glycocalyx (left) and its major components (right). Glycoproteins are seen attached to basal endothelial cells. GAGs are seen branching off from anchor proteoglycans and soluble proteoglycans which are incorporated with hyaluronic acid (HA), endothelial cell superoxide dismutase (ec-SOD), and antithrombin-III (AT III). These components form the endothelial glycocalyx that functions as a barrier between blood plasma and the endothelium and exerts various roles in plasma and vessel wall homeostasis (Reitsma et al. 2007).

Glycoproteins' general structure contains acidic oligosaccharides, such as heparan sulfate, and terminal sialic acids, which contribute to the overall negative charge of the glycocalyx (Weinbaum et al. 2007). In the eGC, sialic acids, such as N-acetylneuraminic acid (Neu5Ac), are terminal residues on glycoproteins and glycolipids. The second components of the glycocalyx "backbone" are the proteoglycans. While glycoproteins have shorter, branched oligosaccharide chains and play roles in cell signaling and adhesion, proteoglycans have long, unbranched glycosaminoglycans (GAG) chains, contributing to their structural support and regulation of vascular permeability. Proteoglycans consist of a core protein to which sulphated GAGs are covalently linked (Milusev et al. 2022). Variations in core proteins include their size, the number of GAGs attached to them, and whether they are bound to the endothelial membrane (Reitsma et

al. 2007). Luminally, the glycocalyx is composed of soluble secreted proteoglycans and GAGs. There are five groups of GAGs: heparan sulfate, chondroitin sulfate, dermatan sulfate, keratan sulfate, and hyaluronan, all outlined in Figure 2 (Reitsma et al. 2007).

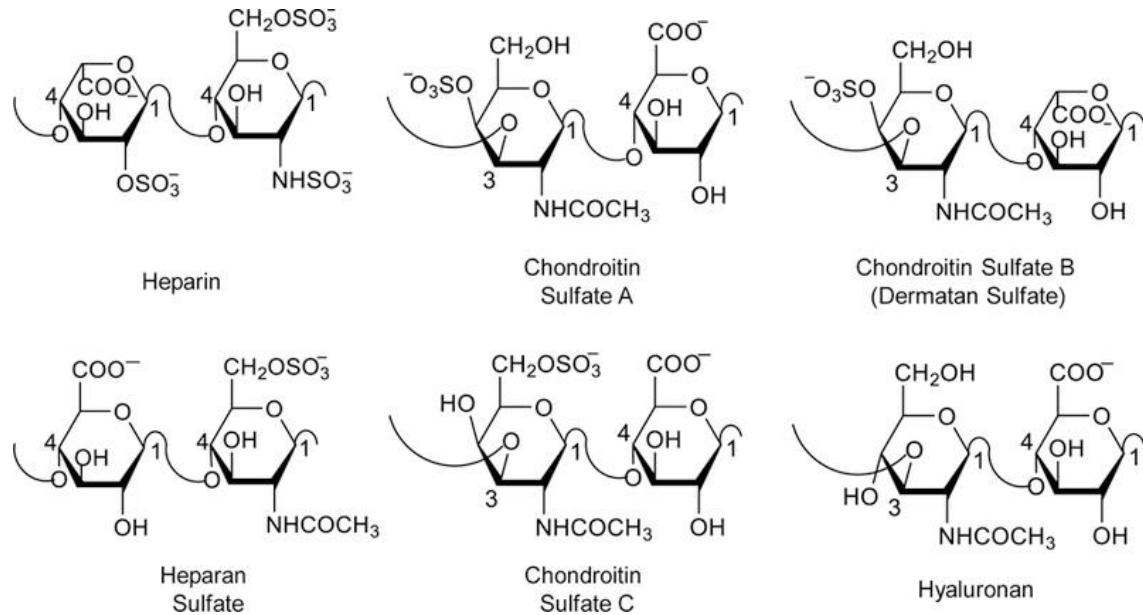


Figure 2. The chemical structures of the main repeating disaccharide units and glycosidic bonds in GAGs. GAGs shown include heparin/heparan sulfate, chondroitin sulfates, hyaluronic acid/hyaluronan, and keratan sulfates. Hyaluronic acid stands out as the only GAG devoid of sulfate groups. The chemical structures of keratan sulfates are not provided (Afosah and Al-Horani 2020).

In the vasculature, heparan sulfate proteoglycans constitute around 90% of the total proteoglycans within the glycocalyx, with chondroitin sulfate/dermatan sulfate being the second most abundant (Oohira et al., 1983; Reitsma et al., 2007). Each GAG molecule can attach to the proteoglycan anchors and be sulfated or acetylated to varying extents. The sulfation of GAGs is a principal factor in determining the negative charge density of the molecule (Volpi 1999). The composition of the membrane-bound mesh of proteoglycans, glycoproteins, and glycosaminoglycans is dynamic. Additionally, the composition of associated plasma proteins and soluble glycosaminoglycans undergoes constant replacement, with no distinct boundary between locally synthesized and associated elements. Identifying clear compositional differences within the

glycocalyx, spanning from the endothelial membrane to the vascular lumen, is difficult. Instead, it appears that the endothelial glycocalyx resembles a complicated, self-assembling mesh of various polysaccharides (Reitsma et al. 2007). A dynamic equilibrium exists between the layer of soluble components of the ESL and the flowing blood, continuously affecting the composition and thickness of the glycocalyx. Several factors can influence the eGC including shear stress, inflammation, diet, various disease and more. Regulated by endothelial cells, ESL volume and composition are highly dependent on its local microenvironment in the vasculature (Reitsma et al. 2007).

ESL in mechanotransduction

One important function of the ESL is to detect alterations in blood flow and subsequently regulate blood vessel diameter to accommodate changes in flow (Reitsma et al. 2007). The endothelium, and thus the ESL, is in constant contact with mechanical forces caused by blood flow, mainly characterized as shear stress. The glycocalyx plays a major role in the mechanotransduction of shear stress signals to the endothelium (Pahakis et al. 2007). Experiments conducted by Florian et al. (2003) and Foote et al. (2023) involved enzymatic degradation of specific components of the glycocalyx using heparinase and neuraminidase. Their findings revealed that degradation of these known glycocalyx components led to a significant decrease in mechanotransduction, as evidenced by a marked reduction in nitric oxide (NO) production and flow-dependent vasodilation.

The glycocalyx is initially involved in the mechanotransduction of shear stress within blood vessels. Tarbell and Pahakis (2006) introduced a conceptual wind-in-the-trees model. This model suggests that GAGs act as drag sensors, transferring force from shear stress to core proteins.

These core proteins then transmit the force to either the plasma membrane or the cytoskeleton within the ESL. Weinbaum et al. (2003) further described that the forces dissipated across the glycocalyx impose a torque on the stiff core proteins. This signal is then transmitted to the actin cortical cytoskeleton via transmembrane domains, thus converting the sheer force into a mechanically stimulated intracellular signal (Cosgun et al. 2020). Further supporting the role of ESL in mechanotransduction, Dragovich et al. (2016) also concluded that shear-mediated NO production was dependent on the presence of both heparan sulfate (HS) and hyaluronic acid (HA) in the endothelial glycocalyx (eGC), as the removal of HS and/or HA lead to a significant decrease in NO production.

eNOS/NO/cGMP vasodilatory pathway

In response to sheer stress on the endothelium, NO is produced by endothelium nitric oxide synthase (eNOS). NO is a highly lipophilic, hyper-reactive, diffusible free radical gas with a relatively short half-life in the blood (Qian and Fulton 2013). As a lipophilic, reactive gas, NO can easily diffuse across multiple cellular membranes and interact with many different cellular and extracellular targets including those involved in vasodilation (Qian and Fulton 2013). eNOS, a bi-domain enzyme, homodimerizes to enable its enzymatic function. Each monomer comprises an N-terminal oxygenase domain with binding sites for L-Arg, heme, zinc, and tetrahydrobiopterin (BH₄), as well as a central calmodulin-binding region. Additionally, it contains a C-terminal reductase domain with nicotinamide adenine dinucleotide phosphate (NADPH), flavin adenine dinucleotide (FAD), and flavin mononucleotide (FMN) binding sites (Janaszak-Jasiecka et al., 2023). NO synthesis occurs from L-arginine and molecular oxygen, with eNOS transferring electrons from NADPH to the heme in the oxygenase domain (Förstermann and Sessa, 2012).

BH₄, a crucial cofactor, binds to the oxygenase domain along with molecular oxygen and L-arginine. Electrons from NADPH reduce and activate O₂ while oxidizing L-arginine to L-citrulline and NO at the heme site (Förstermann and Sessa, 2012). Basically, O₂ trades one of its oxygens for nitrogen from L-arginine forming L-citrulline and NO.

NO freely diffuses into vascular smooth muscle cells and activates the guanylyl cyclase (sGC)—cyclic guanosine monophosphate (cGMP) signalling pathway (Qian and Fulton 2013). In this pathway, sGC is bound with high affinity to NO which catalyzes the formation of cGMP from guanosine triphosphate (GTP). cGMP then activates downstream effector systems such as protein kinases, phosphodiesterases, and ion channels. These effector systems stimulate the extrusion of Ca²⁺ from the smooth muscle and cellular hyperpolarization to cause smooth muscle relaxation and vasodilation of the blood vessel (Patik et al. 2021). Through this pathway, the ESL can sense changes in blood flow and activate enzymes that release important vasodilators, like NO, that adjust the size of the vessel according to the mechanical shear stress applied to it. However, eNOS activation is preceded by many other cellular processes. As described in a review by Da Silva et al. (2021), and illustrated in Figure 3, the endothelial relaxation response initiates when vasodilator agents bind to membrane receptors on endothelial cells or through shear stress (which alternatively triggers PI3K/AKT-dependent eNOS phosphorylation). Upon activation of membrane G-protein coupled receptors (GPCR), phospholipase C (PLC) is activated, leading to increased diacylglycerol (DAG) and inositol 1,4,5-trisphosphate (IP3) production. IP3 stimulates calcium release from the cytoplasmic reticulum of the endothelial cell, elevating cytoplasmic Ca²⁺ levels. This rise in Ca²⁺ activates calmodulin, which subsequently activates eNOS to produce NO. The specific functions of active cGMP include phosphorylation of myosin light chain kinase (MLCK)

and activation of potassium channels and myosin light chain phosphatase (MLCP). Collectively, these actions induce relaxation in vascular smooth muscle cells and causes vasodilation.

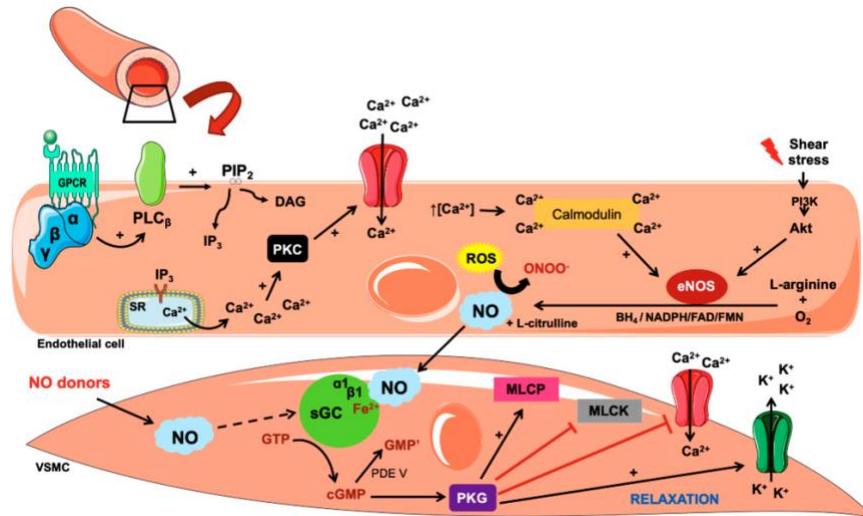


Figure 3. Diagram of NO pathway from synthesis to relaxation. NO prompts VSMC relaxation by activating GPCRs, triggering PLC, leading to calcium release. Calcium and other cofactors activate eNOS, producing NO. NO binds to sGC in VSMC, generating cGMP, which activates PKG, promoting VSMC relaxation. Shear stress can also activate eNOS independently of GPCR (da Silva et al. 2021).

Disruption of these processes, such as eNOS uncoupling and ESL damage, can lead to endothelial dysfunction, which is the first step in CVD development (Gallo et al. 2022; Hadi et al. 2005; Widmer and Lerman 2014). One definition of endothelial dysfunction is an imbalance in NO production and consumption, where consumption is favoured over production, leading to reduced NO levels (Widmer and Lerman 2014). This can lead to an inability of the ESL to sense changes in the blood vessel and regulate its diameter. Endothelial dysfunction can be attributed to high oxidative stress and inflammation, which alter NO metabolism and can lead to global vasoconstriction (Hadi et al. 2005; Jay Widmer and Lerman 2014). Transient dysfunction can also be caused by mechanical shear stress or other factors that damage the sensory components of the

eGC (Kröpfl et al. 2021). Additionally, endothelial dysfunction is characterized by a shift towards reduced vasodilation, smooth muscle cell proliferation, platelet adhesion and activation and proinflammatory and prothrombic state within the arterial wall. This state favours all stages of atherogenesis and increases CVD risk (Gallo et al. 2022).

ESL as a non-osmotic salt buffer

Another crucial role of the ESL in hypertension and inflammation is its function as a buffer for dietary Na^+ , which helps maintain blood vessel function and vascular health (Reitsma et al., 2007). The traditional two-compartment model of Na^+ homeostasis, which involves regulation through storage in plasma and kidney-mediated water retention and release, has been expanded to incorporate Na^+ storage beyond plasma levels. (Wenstedt et al. 2021). These alternate compartments include the skin, muscle, and blood vessel wall which can vary in Na^+ storage with dietary intake. Na^+ storage by the ESL is facilitated by the net negative charge of the glycocalyx, which is determined by varying sulfation of GAGs. Negatively charged GAGs are thought to retain passing Na^+ through electrostatic interactions between the positive charge of Na^+ and the negative charge of the GAGs located in the eGC (Olde Engberink et al. 2014).

Several studies have investigated the relationship between GAG sulphation and synthesis, and Na^+ storage. GAGs in the ESL include heparan sulfate, chondroitin sulfate, dermatan sulfate, keratan sulfate, and hyaluronan (Olde Engberink et al. 2014). Using differing Na^+ loading conditions in rats, Titze et al. (2004) found that non-osmotic Na^+ storage correlated with specific changes in GAG metabolism, where increasing skin Na^+ was paired with increasing GAG content. They also concluded that dietary NaCl loading coincided with increased chondroitin synthase mRNA content in the skin, which is a key component of the GAG structure of the ESL (Djerbal et

al. 2017). In a human study by Selvarajah et al. (2017), dietary salt loading similarly increased Na^+ storage in the skin. They noticed differences between sexes in salt storage and suggested that men's thicker skin, potentially containing higher levels of dermal glycosaminoglycans, may act as a more effective buffer for dietary Na^+ .

The role of the ESL in Na^+ buffering has significant clinical implications in disease states associated with ESL damage and salt intake. Diabetes mellitus and chronic kidney disease are frequently linked with ESL damage and blood volume overload (Olde Engberink et al. 2019). This suggests that ESL damage leading to the inability of the ESL GAGs to store Na^+ may play a role in maintaining normal volume regulation. In these diseases, the absence of Na^+ storage manifests as volume overload (Olde Engberink et al. 2019). Insights into Na^+ regulation challenge our understanding of blood pressure control and hypertension, especially regarding the impact of Na^+ intake, known as Na^+ sensitivity. Previous research mainly focused on renal function, assuming impaired Na^+ excretion as the cause of Na^+ sensitivity. However, recent findings indicate a broader regulation beyond the kidneys (Olde Engberink et al. 2019). The skin interstitium and extracellular space are emerging as potential influencers of Na^+ sensitivity. A disrupted or salt-overloaded ESL, with diminished Na^+ buffering capacity, permits increased Na^+ transport into endothelial cells. This impairs the endothelium, resulting in elevated reactive oxygen species (ROS), reduced antioxidant defences, endothelial cell stiffening, and additional damage to the endothelial glycocalyx (Olde Engberink et al., 2019; Patik et al., 2021).

Salt-induced increases in oxidative stress impair endothelial function

As mentioned previously, oxidative stress refers to an imbalance of ROS and antioxidant activity. In particular, superoxide (O_2^-) can impair NO-mediated vasodilation by readily binding

NO, reducing its bioavailability and forming the free radical peroxynitrite (ONOO⁻) (Landmesser et al. 2005; Patik et al. 2021). Both O₂⁻ and ONOO⁻ can then oxidize the eNOS cofactor BH₄, resulting in the uncoupling of eNOS and generation of O₂⁻ rather than NO. This increase in O₂⁻ and ONOO⁻ by eNOS uncoupling represents a positive feedback loop of endothelial impairment through continuous removal of NO for vasodilation and accelerated production of O₂⁻ from eNOS uncoupling (Figure 4) (Tran et al. 2022).

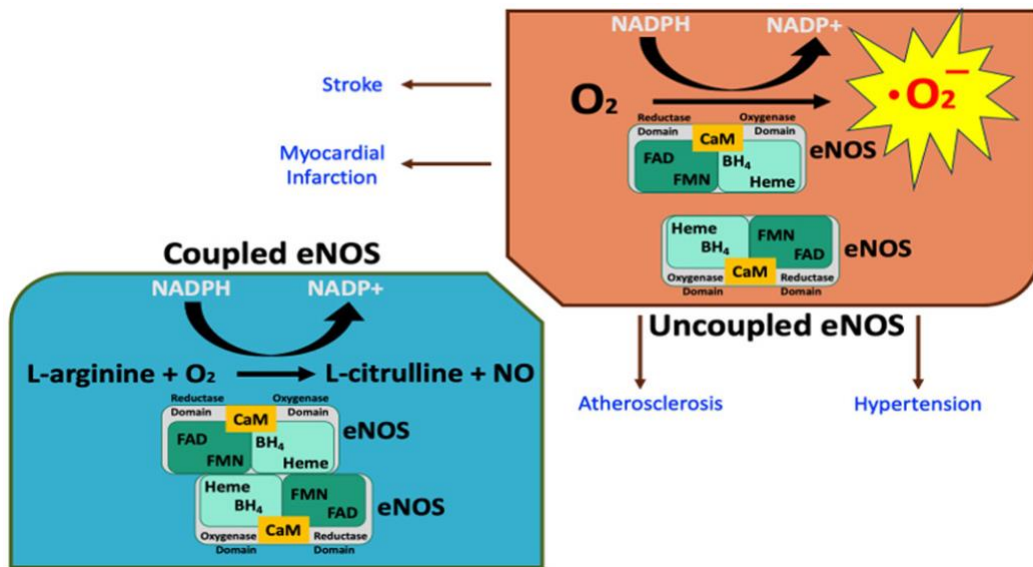


Figure 4. Diagram of coupled versus uncoupled eNOS showing that uncoupled eNOS can generate O₂⁻, a highly toxic super radical. Uncoupled eNOS can subsequently contribute to the development of various CVDs (Tran et al. 2022).

An increase in oxidative stress due to high salt has been found in many studies in rats and humans. Lenda et al. (2000) found that an increase in ROS from a high Na⁺ diet-induced endothelial dysfunction that was restored in the presence of the O₂⁻ scavenger superoxide dismutase (SOD). In a human study by Jablonski et al. (2013) a low-Na⁺ diet significantly increased brachial artery flow-mediated dilation (FMD), indicating improved endothelial function. This was accompanied by increased NO and BH₄ bioavailability and reduced oxidative stress. They also found that supplementation with vitamin C, a well-established antioxidant, improved

brachial FMD potentially by restoring the redox balance and preventing oxidative stress-related dysfunction. High salt intake has also been linked to the inhibition of antioxidant defences in the endothelium, primarily through the reduced SOD protein expression. SODs catalyze the dismutation of O_2^- into molecular oxygen and hydrogen peroxide (H_2O_2). This process reduces O_2^- levels, which can damage cells at high concentrations (Younus 2018). Typically studied in rats, both activity and expression of SOD isoforms were reduced with high salt diets (Patik et al. 2021).

Several studies have also investigated the effects of a high-salt diet on NADPH oxidase another contributor of O_2^- . NADPH oxidases are recognized as the primary generators of O_2^- in the vasculature. In various conditions like diabetes, hypertension, smoking, obesity, and aging, both the increased expression and activity of NADPH oxidases exist. The activation of NADPH oxidases plays a significant role in cardiovascular disease development (Janaszak-Jasiecka et al. 2023). Numerous studies suggest that high salt intake induced greater NADPH oxidase expression (Guers et al. 2019; Kitiyakara 2003) or activity (Lenda and Boegehold 2002; Zhu et al. 2007) in rat arteries contributing to increased oxidative stress. Various factors, including the exercise immune response and excess dietary salt, can cause increased oxidative stress and redox imbalances leading to ESL damage and endothelial dysfunction (Figure 5) (He et al. 2016; Patik et al. 2021).

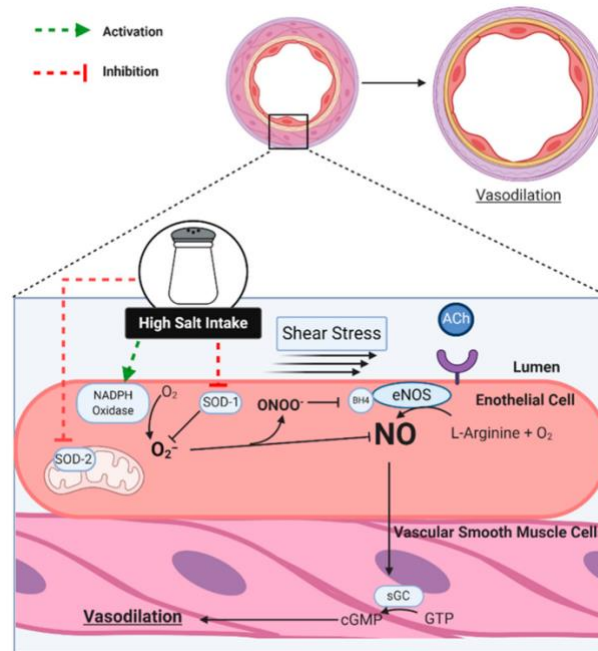


Figure 5. Summary of the oxidative stress-related pathways that excess dietary salt can disrupt causing endothelial dysfunction. Elevated dietary Na^+ levels increase O_2^- production by activating NADPH oxidase and inhibiting SOD-1 and mitochondrial SOD (SOD-2). NO reacts readily with O_2^- , preventing its diffusion into vascular smooth muscle. Although not shown, the resulting ONOO^- oxidizes BH_4 , which leads to uncoupling of eNOS, leading to further reductions in NO and increases in O_2^- (Patik et al. 2021).

Salt induces endothelial cell stiffening and glycocalyx damage

High dietary Na^+ intake may diminish NO release by altering the mechanical properties of endothelial cells. Several studies have documented endothelial cell stiffening and ESL damage when endothelial cells are exposed to elevated Na^+ concentrations (Korte et al. 2011; Lenda et al. 2000; Oberleithner et al. 2011; Oberleithner et al. 2007; Olde Engberink et al. 2019; van Golen et al. 2014). Oberleithner et al. (2007) cultured endothelial cells exposed to a Na^+ bath which increased stiffness and reduced NO release. Korte et al., (2011) expanded on Oberleithners 2007 study finding that this effect was caused by the opening of epithelial Na^+ channels (ENaC), leading to Na^+ entry, and subsequent cell swelling and stiffening. Another study by Oberleithner et al.

(2011) demonstrated that prolonged exposure to high extracellular Na^+ concentrations resulted in a 50% reduction in eGC height and a 130% increase in ESL stiffness. Oberleithner et al. (2011) also observed a reduction in heparan sulfate residues, a major component of the eGC, by 68%, leading to eGC destabilization and collapse. These studies suggest that ESL damage may increase Na^+ entry into endothelial cells, potentially contributing to endothelial dysfunction and arterial hypertension in individuals with high salt intake (Korte et al. 2011; Oberleithner et al. 2011; Oberleithner et al. 2007). The combination of eGC damage and endothelial cell stiffening diminishes the mechanotransduction of shear stress into NO release, further exacerbating endothelial dysfunction (Patik et al. 2021). In summary, excess salt consumption can significantly impair endothelial function by attenuating NO release and damaging the endothelial glycocalyx, as shown in Figure 6.

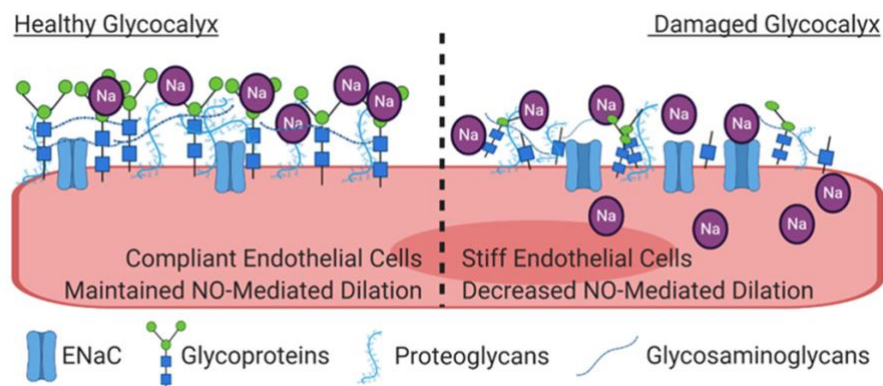


Figure 6. Comparing a healthy and damaged ESL, where damage to the eGC allows infiltration of Na^+ into endothelial cells causing decreased NO-mediated dilation and endothelial cell stiffness. To the left, the healthy glycocalyx acts as a protective barrier between the plasma and the endothelial cell, buffering positively charged Na^+ . Conversely, elevated plasma Na^+ levels on the right result in glycocalyx damage, allowing increased Na^+ access to ENaC on the endothelial surface, consequently raising intracellular Na^+ concentrations. In such instances, cellular stiffness increases, and the conversion of shear stress into NO release is diminished (Patik et al. 2021).

Exercise-induced ESL damage

Exercise may be another factor that can transiently impair endothelial function, likely through its systemic and local effects that degrade the ESL. Typically, a bout of exercise increases blood flow to working muscles, whilst reducing blood flow to non-working tissues (Sarelius and Pohl 2010). This increased blood flow usually dilates large and small arteries through the ESL's ability to control the release of NO (Pahakis et al. 2007).

Endurance workouts or mainly aerobic exercise are widely recognized for triggering the overproduction of ROS from heightened metabolism (He et al. 2016). This phenomenon leads to oxidative stress and associated injuries. Studies suggest that endurance exercise can result in a 1-3-fold increase in O_2^- levels during muscle contraction (Sakellariou et al. 2013). The increase in ROS resulting from exercise may lead to reductions in endothelial function through pathways involving increases in oxidative stress. It should be noted, however, that regular or moderate exercise has been shown to enhance antioxidant defence and endothelial function (He et al. 2016). It is acute bouts of intense exercise that can transiently reduce endothelial function through the overproduction of ROS (Higashi, 2015).

Exercise-induced increases in local blood flow have also been found to disrupt the ESL through shear stress-induced glycocalyx damage. This disturbance can lead to transient reductions in FMD when measured using the ultrasound technique. In fact, strenuous exercise impairs endothelial function and researchers suggest that during exercise the ESL can be shed (Hahn et al. 2021; Steinach et al. 2022). Lee et al. (2019) found that after a cycling exercise at 70% VO_2 max for 45 minutes, glycocalyx components increased in the serum. They concluded that the increase in serum concentrations of glycocalyx components may have been due to acute shedding caused by increased blood flow in the vessels Grandys et al. (2023) similarly supported glycocalyx

shedding as a cause of a marked decrease in FMD in overtrained female track athletes who had significantly higher serum concentrations of HA and syndecan-1 (SDC-1).

Damage to the ESL may liberate stored Na⁺

Once the ESL is shed, it may liberate stored Na⁺ from the ESL, enabling it to enter the endothelium and induce endothelial dysfunction as described above (Patik et al. 2021). Considering the important role of ESL GAGs in salt storage, and the potential degradation caused by prolonged excess salt intake and acutely by strenuous exercise, exercise-induced damage to the ESL may interact with the effects of excess salt, amplifying endothelial damage and dysfunction (Hahn et al. 2021; Kröpfl et al. 2021; Olde Engberink et al. 2019; Steinach et al. 2022). Excess salt damaging the ESL or local blood flow changes from exercise could allow greater transport of salt directly into the endothelium, further exacerbating endothelial cell stiffening and disruption of the eNOS/NO/cGMP dilation pathway (Korte et al. 2011; Oberleithner et al. 2011; Patik et al. 2021). The transient imbalance of ROS from exercise may independently cause endothelial dysfunction by increasing oxidative stress-related disruption of the vasodilatory pathway. Measuring endothelial dysfunction through FMD can allow us to quantify each of these factors that may affect ESL and endothelial dysfunction, both individually and in conjunction with each other. However, whether the blood flow directly causes ESL shedding or if other effects of exercise, such as the activation of the immune system, trigger this process, remains unknown.

Effects of salt and exercise on immune response

Besides the effects of excess salt and exercise on endothelial damage, there are also changes in circulating immune cell populations that occur immediately post-exercise and

following excessive salt loading (Li et al. 2022). It is well understood that during and immediately after exercise, there are significant changes in the composition and number of blood leukocytes (Peake et al. 2017). All major leukocyte subpopulations tend to increase in number during exercise due to hemodynamic shear stress and/or catecholamines acting on leukocyte β_2 -adrenergic receptors (Peake et al. 2017). These circulating immune cells include neutrophils, monocytes, and lymphocytes, which undergo various alterations both during exercise and during periods of excess salt loading. These alterations could affect their contributions to oxidative stress and, therefore, endothelial dysfunction.

Neutrophils

Neutrophils experience suppressed activity with excess salt intake, including suppression of degranulation, O_2^- production, phagocytosis, adhesion, and migration (Li et al. 2022). In human neutrophils, Krampert et al. (2021) concluded that high salt prevented excessive ROS production, which decreased their antimicrobial potential but curtailed ROS-mediated damage. This implies that while salt may hinder neutrophils' ability to contribute to oxidative stress to combat pathogens salt may also prevent damage to the ESL by hindering ROS production. Conversely, Mazzitelli et al. (2022) reported that the effect of salt on neutrophil activity was dependent on exposure time. Initially, neutrophils under high salt conditions were inhibited, showing a lack of response to conventional agonists such as lipopolysaccharide (LPS), the chemotactic peptide fMLP, or Zymosan. However, exposure to high concentrations of salt for longer periods resulted in the activation of neutrophil inflammatory responses and an increased response to conventional agonists.

While investigating the links between exercise-induced neutrophilia and blood oxidative stress, Quindry et al. (2003) found significant blood oxidative stress immediately after maximal intensity exercise. They also observed neutrophilia and a subsequent increase in neutrophil-generated O_2^- . However, Quindry et al. (2003) stressed that other potential sources for oxidative stress cannot be ruled out, limiting their findings. The effects of salt and exercise on neutrophil activity in the context of oxidative stress are yet to be studied.

Monocytes and macrophages

A high salt diet can also increase circulating monocytes in mice and humans and induce the formation of pro-inflammatory human monocytes, which play a key role in the immune response by promoting inflammation (Li et al. 2022; Austermann et al. 2022). These monocytes are characterized by their ability to produce and release pro-inflammatory cytokines, such as tumour necrosis factor-alpha (TNF- α), interleukin-1 beta (IL-1 β), and interleukin-6 (IL-6), NO and ROS upon activation (Li et al. 2022; Austermann et al. 2022). Wenstedt et al. (2019) demonstrated that a high salt diet increased C-C chemokine receptor type 2 (CCR2) expression on monocytes in vitro and in vivo, coinciding with increased plasma monocyte chemoattractant protein-1 (MCP-1), increased salt-induced transendothelial migration of monocytes, and increased skin macrophage content. Wenstedt et al. (2019) also found macrophages demonstrated an increase in pro-inflammatory phenotype after salt exposure. This pro-inflammatory priming of both monocytes and macrophages, as well as CCR2, has been linked to the development of hypertension and atherosclerosis, which is associated with ESL damage and endothelial dysfunction (Wenstedt et al. 2019; Xiao and Harrison 2020). Further supporting the effects of high salt on macrophages, Zhang et al. (2015) found that high salt can induce a shift in macrophage phenotype, characterized

by enhanced pro-inflammatory and suppressed anti-inflammatory gene expression. Wonner et al. (2016) examined the exercise effects on monocytes and observed a significant mobilization of CD14⁺CD16⁺ pro-inflammatory monocytes even after a small one-minute bout of strenuous exercise. While reviewing the clinical impacts of Na⁺ storage, Olde Engberink et al. (2019) described how monocytes, which seem attracted to high skin Na⁺ concentrations, play a crucial regulatory role in Na⁺ homeostasis. They further explained that once in the skin, macrophages modulate vascular endothelial growth factor-C (VEGF-C)–mediated cell increases of lymph vessels, which is considered the principal process of mobilization of excessive Na⁺ from the skin. Basically, macrophages control the growth of cells within lymph vessels in the skin, which helps in eliminating excess Na⁺ from this tissue.

Natural killer cells

During and following exercise, Natural killer (NK) cell levels rise in peripheral blood. This increase is attributed to the release of cytokines during muscle contraction, which promotes the proliferation, maturation, and activation of NK cells (Quintana-Mendias et al., 2023). Additionally, exercise induces the release of catecholamines, mobilizing epinephrine-dependent NK cells (Quintana-Mendias et al., 2023). Moreover, heightened blood flow can stimulate circulating NK cells by activating NK reservoirs located in the vascular endothelium (Quintana-Mendias et al., 2023). Although the dysregulation of NK cell activation and development has been investigated during high salt diets, their contribution to oxidative stress has yet to be reported.

The effects on immune cell populations vary depending on the cell type. While neutrophils and macrophages may contribute to inflammation and oxidative stress during exercise and high salt diets, there is less evidence regarding the role of NK cells in generating ROS (Quindry et al.

2003; Zhang et al. 2015). Monocytes might also play a crucial role in removing excess Na⁺ from the skin, but it is unclear whether this process is enhanced or diminished during strenuous exercise leading to monocytosis (Olde Engberink et al. 2019).

Exercise as an immune system adjuvant

During short-duration moderate to high-intensity workouts lasting less than 60 minutes, tissue macrophages display antipathogen activity, and there is increased circulation of immune components such as immunoglobulins, anti-inflammatory cytokines, neutrophils, NK cells, cytotoxic T cells, and immature B cells (Nieman and Wentz 2019). These elements are crucial for immune defence and metabolic health. Additionally, short-duration moderate exercise does not lead to high levels of stress hormones or proinflammatory cytokines, unlike high-intensity or prolonged exercise, which preserves immune cell function and reduces inflammation over time (Nieman and Wentz 2019).

Objectives

In this study, we aim to investigate whether a high-salt diet induces endothelial dysfunction and whether changes in blood flow that induce disruption of the endothelial surface layer can exacerbate this dysfunction. To examine these mechanisms, we will use lower-body exercise as a stimulus to induce local lower limb ESL disruption. Additionally, we will assess immune system activation and endothelial function measures in the non-exercised upper limbs to identify whether changes are immune-related or systemic. To achieve this, the strenuous exercise bout involving cycling, which can stimulate a whole-body immune response characterized by an increase in leukocyte cell counts and other inflammatory markers (Akhtari-Shojaei 2011). Cycling will primarily increase blood flow to the legs whereas arm blood flow will remain relatively stable thus localizing flow-induced ESL disruption to the legs. By comparing the dilation in the arms to that

in the legs before and after exercise, we can determine whether local blood flow and oxidative stress or the immune response contribute to ESL disruption. Additionally, we will examine whether the effects of salt exacerbate or blunt any observed endothelial dysfunction.

METHODS

Ethics

Ethics approval was granted by the Thompson Rivers University ethics committee. All participants were informed of study procedures and risks and signed written consent forms to partake in the study which were witnessed and signed by the investigators.

Participants

Participants were pre-screened to ensure they all met the inclusion criteria and completed a Physical Activity Readiness + (PAR-Q+) (Bredin et al., 2013). Participants did not have a history of cardiovascular disease, diabetes, blood-related diseases, or other cardiovascular risk factors. Participants were non-smokers and did not have any known metabolic disorders. Before testing was conducted, participants were instructed to avoid physical activity including cycling, running, and resistance exercise 24 hours before testing. Participants were also instructed to avoid consumption of alcohol, marijuana, and any other non-prescription drugs 24 hours before testing. Participants were additionally instructed to avoid caffeine and not eat four hours before testing on the testing days.

Determining exercise capacity

Exercise capacity testing involved a graded exercise test on a cycle ergometer (Garmin TacX cycle ergometer, Garmin Ltd. US). At the beginning of each Exercise capacity test, a gas

and volume calibration was performed according to the manufacturer's instructions on the Quark CPET metabolic cart (COSMED, Italy). The ramp exercise bout involved a five-minute warm-up at 50 Watts followed by an increased work rate of 25 watts per minute. The incremental ramp exercise was controlled through TacX Bluetooth software (TacX cycle ergometer, Garmin Ltd. US) to actively control resistance and monitor and record pedal speed. Participants maintained 70 rotations per minute (RPM) pedal cadence and continued the exercise bout until volitional fatigue. Breath-by-breath data was measured and monitored using the Quark CPET metabolic cart (COSMED, Italy) and analyzed to identify ventilatory thresholds (VT1 and VT2). VT1 and VT2 were identified using a modified V-slope method (Beaver et al. 1986). This method involved analyzing plots of $\dot{V}E/\dot{V}CO_2$, $\dot{V}E/\dot{V}O_2$, $\dot{V}CO_2/\dot{V}O_2$, PET_{CO_2} and PET_{O_2} , and respiratory quotient (RQ) over time.

Ventilatory threshold 1

Ventilatory threshold 1 (VT1) was found by combining points on the graphs to find the most likely wattage that resulted in achieving VT1. During incremental exercise below the VT1, the amount of carbon dioxide (CO_2) delivered to the lungs increases linearly with oxygen uptake ($\dot{V}O_2$). However, once above the VT1, the rate of CO_2 output ($\dot{V}CO_2$) starts to increase more rapidly in relation to $\dot{V}O_2$ (Beaver et al., 1986; Solberg et al., 2005). This change in CO_2 output relative to O_2 consumption can be seen graphically at the intersection point of the two linear portions of the $\dot{V}CO_2/\dot{V}O_2$ curve (as seen in Figure 7). Additionally, this point can be cross-referenced with the RQ by time graph. RQ is the ratio of carbon dioxide produced to oxygen consumed which provides insight into the metabolic substrates utilized during exercise (Kakutani et al. 2018). As exercise intensity increases, there is a gradual increase in metabolism through

anaerobic pathways alongside aerobic pathways, characterized by an increase in RQ. The point at which RQ begins to rise indicates a sharp increase in anaerobic metabolism as intensity increases (Solberg et al. 2005). RQ over time can be used to validate the VT1 value found using the $\dot{V}CO_2/\dot{V}O_2$ graph, where the VT1 must be achieved before RQ surpasses a value of 1.0. Figures 7 and 8 illustrate graphs derived from breath-by-breath data collected during an incremental ramp exercise test to find VT1.

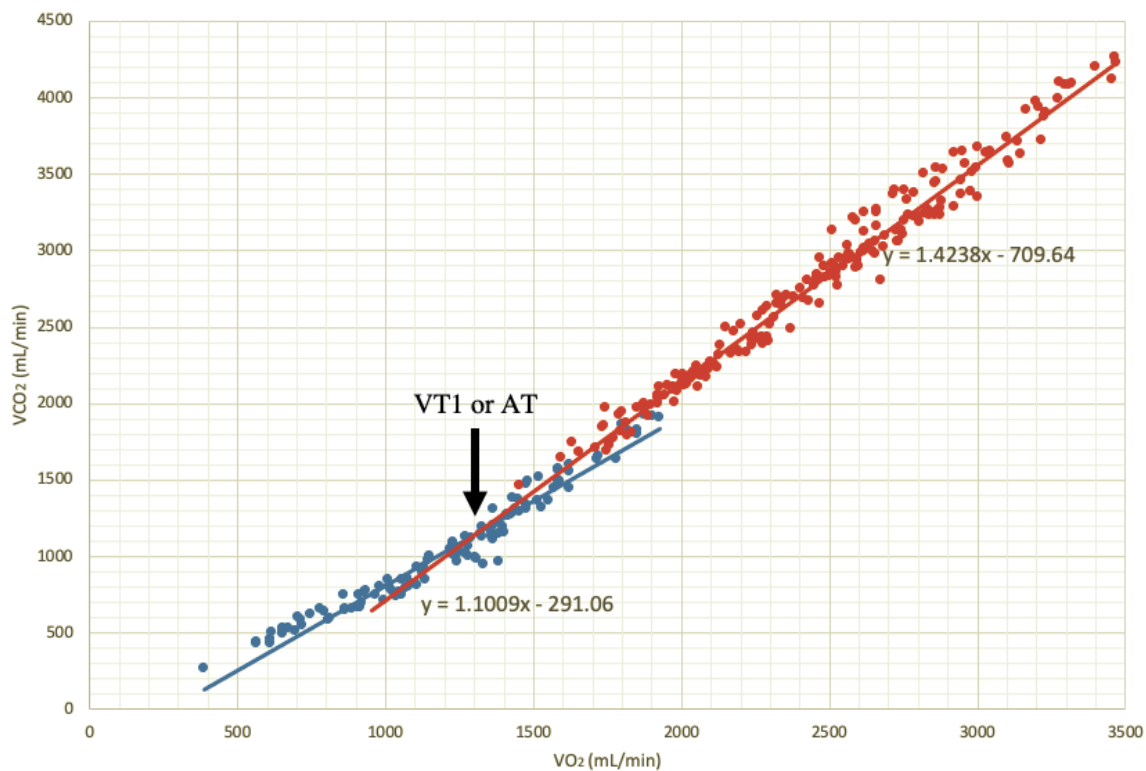


Figure 7. $\dot{V}CO_2$ over $\dot{V}O_2$ graph to identify VT1 through intersection points of linear components. The intersection point of the two linear segments represents VT1. Each point is from breath-by-breath data collected during an incremental ramp exercise test using Quark CPET metabolic cart (COSMED, Italy)

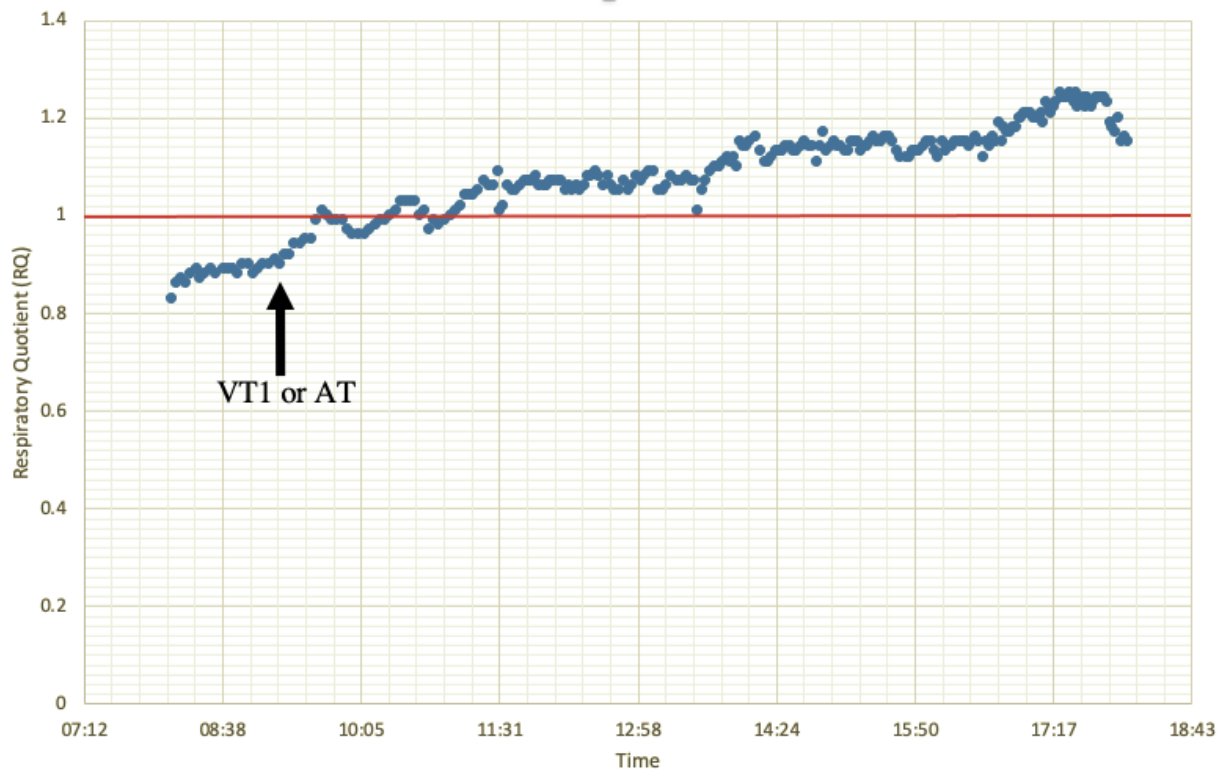


Figure 8. RQ over time to validate VT1 found on the $\dot{V}CO_2/\dot{V}O_2$ graph. The red line represents the threshold RQ of 1.0. Once RQ begins increasing and is below 1.0, VT1 will have been reached.

Minute ventilation (\dot{V}_E) and PET_{O_2} and PET_{CO_2} graphs can also be used to find ventilatory thresholds. VT1 estimations can be verified using the following criteria: 1) The $\dot{V}_E/\dot{V}O_2$ curve begins to rise as the $\dot{V}_E/\dot{V}CO_2$ curve remains flat or decreases, 2) The PET_{CO_2} curve is rising or constant, while the PET_{O_2} curve changes from declining or flat to rising. Estimates of VT1 generally fall between 45% and 65% of individuals measured $\dot{V}O_2$ max, which can also be used as validation (Balady et al. 2010; Davis et al. 1976). Each participant's VT1 was used to calculate the appropriate exercise prescription for subsequent testing sessions. Both individually and in combination, these methods have undergone extensive review and testing to establish their effectiveness in identifying VT1 (Beaver et al., 1986; Davis et al., 1976; Kakutani et al., 2018; Solberg et al., 2005).

Ventilatory threshold 2

Ventilatory threshold 2 (VT2) marks the stage of incremental exercise characterized by a rapid rise in VE compared to $\dot{V}O_2$ (Martini et al., 2022). This surge in VE, resulting from increased respiratory rate and tidal volume, is driven by heightened CO₂ production due to hydrogen ion accumulation with escalating exercise intensity (Martini et al., 2022). While VT1 can be identified as the point where the VE/ $\dot{V}O_2$ curve begins to rise as the VE/ $\dot{V}CO_2$ curve remains flat or decreases, VT2 is identified as the point where VE/ $\dot{V}O_2$ and VE/ $\dot{V}CO_2$ simultaneously increase. VT2 can also be found by examining the $\dot{V}CO_2/\dot{V}O_2$ graph, where a third linear component may appear beyond VT1, intersecting with the second component. However, in practice, identifying this third component can be challenging (Martini et al., 2022). Using the PET_{CO2} over time graph the deflection point of the curve where PET_{CO2} begins to decline can also establish VT2 (Anselmi et al. 2021). Figure 9 illustrates the indices for VT1 and VT2.

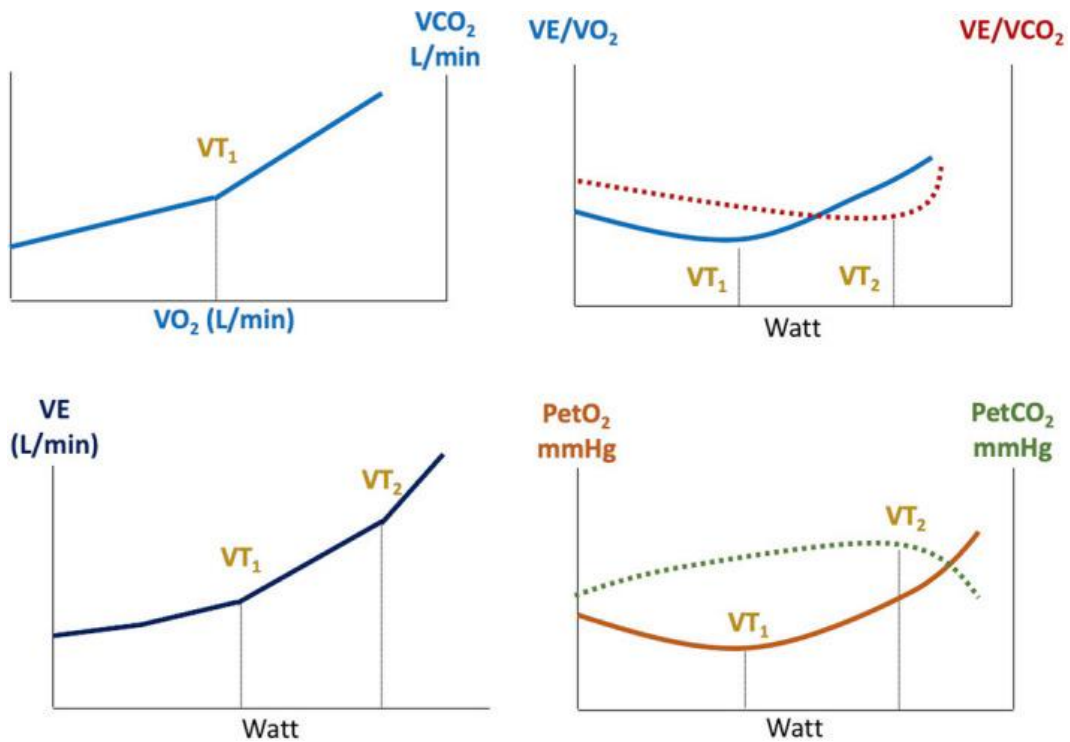


Figure 9. General outline of the identification of the first and second ventilatory thresholds (VT1 and VT2) through cardiopulmonary exercise testing (CPET). This includes a focused examination of parameters such as $\dot{V}O_2$ versus $\dot{V}CO_2$, $\dot{V}E/\dot{V}CO_2$, $\dot{V}E/\dot{V}O_2$, $\dot{V}E$, and PET_{O_2} and PET_{CO_2} panels. "Watt" symbolizes the rising resistance encountered in ramp incremental testing. Although not shown, RQ over time may also be used for the determination of VT1, when it begins rising signalling an increase in anaerobic metabolism and achievement of VT1 (Anselmi et al. 2021).

Generally, VT1 can be achieved within 1–3 minutes of incremental ramp testing, while VT2 may take 10-15 minutes to reach (Rossiter 2011). The desired work rate was calculated as the wattage value 1/3 between the wattage at VT1 and VT2, within the heavy exercise domain. This work rate would cause glycocalyx shedding and immune system activation, but not exhaustive levels of exertion for participants (Sapp et al. 2019; Schlagheck et al. 2020). Several studies have demonstrated that moderate to high-intensity exercise was required to cause glycocalyx shedding, oxidative stress, and immune response (He et al. 2016; Kröpfl et al. 2021; Lee et al. 2019; Peake et al. 2017; Quindry et al. 2003; Quintana-Mendias et al. 2023; Steinach et al. 2022; Wonner et al. 2016).

Experimental design

After completing exercise capacity testing, participants returned to the lab on four separate days for experimental trials. In experimental session one, baseline readings were taken without salt loading. Participants were then given salt or sugar pills (1.15 g) to be taken daily over two weeks. Sugar pills served as the placebo, while salt pills constituted the experimental treatment. Whether placebo or salt pills were given first was randomized for each participant. Participants gradually increased salt intake to 13.8 g per day by consuming 12 pills daily. Experimental session two occurred exactly two weeks after experimental session one, involving the same measurements. Following experimental session two, a two-week washout period was implemented to return participants to baseline levels. Experimental session three reassessed participants' baseline variables. Subsequently, participants resumed salt or sugar pill intake for another two weeks. Experimental session four marked the final testing day, with measurements identical to previous days. Throughout the trial, participants maintained their regular diets and lifestyles. Salt pills were designed to dissolve in the small intestine to minimize adverse effects, reducing the likelihood of early release in the stomach and subsequent nausea. Participants were instructed to consume no more than 3-4 pills at once and to take pills only after eating to mitigate nausea.

Experimental sessions involved continuous blood pressure recording, electrocardiogram (ECG) measurements and ultrasound measurements to assess FMD of popliteal and brachial arteries. Venous blood samples were obtained and analyzed through enzyme-linked immunosorbent assay (ELISA) testing and flow cytometry. Blood pressure was measured using photoplethysmography (PPG). This method of continuous non-invasive arterial pressure monitoring (CNAP) uses the volume clamp technique in which an infrared light is shone through the middle or fourth finger whilst a cuff inflates and deflates to keep blood volume constant. These

changes in cuff pressure are proportional to arterial blood pressure and calibrated to oscillometrically obtained brachial blood pressure. Since light is absorbed by blood, changes in blood flow can be detected by PPG sensors as changes in the intensity of light through the finger cuffs. After participants were instrumented, they were instructed to lie in a supine position at rest for approximately 20 minutes to ensure resting conditions. Once participants finished their rest period, a baseline FMD was determined at the brachial, and popliteal arteries. Additionally, a venous blood sample of 5 mL was obtained from an antecubital vein and placed in an EDTA tube. An aliquot of 1 mL of blood was taken from the 5 mL sample for flow cytometry preparation and the rest of the 4 mL were centrifuged at 2500 g for 10 minutes. Two hundred and fifty μ L of plasma was then distributed in six Eppendorf tubes to be analyzed for glycocalyx components. Once baseline data collection was completed, the 45-minute exercise bout began at the previously determined work rate (1/3 between VT1 and VT2). Immediately after exercise, blood was drawn and FMD was assessed at the brachial and popliteal arteries.

Flow-mediated dilation

FMD was measured at the brachial and popliteal arteries using an EPIQ 5 Ultrasound system (Phillips, US). The FMD protocol consisted of a baseline measurement of artery diameter with no peripheral ischemia followed by an assessment of dilation after cuff deflation (Rosenberry & Nelson, 2020). Recordings included 15 seconds of resting artery diameter, 15 seconds before pressure cuff release, and two minutes immediately post-pressure cuff release. Ischemia of the forearm or calf was induced downstream of the artery of interest by inflation of a blood pressure cuff to >200 mmHg for five minutes. Releasing the pressure cuff triggers an immediate surge in blood flow through the brachial or popliteal artery, initiating vasodilation in the blood vessels

(Rosenberry & Nelson, 2020). Ultrasound recordings were taken in 15- and 30-second durations. Video clips were transferred using a USB to be analyzed through CaroLab software (Zahnd et al. 2017) and Microsoft Excel 2016 (Microsoft Corporation, 2016).

Using CaroLab software, arterial walls were identified and tracked throughout the video clips to identify baseline vessel diameter and peak vessel diameter. Baseline diameter was measured over 15 heart cycles and peak diameter was measured over 3 heart cycles. The number of frames analyzed for 15 and 3 heart cycles was dependent on the heart rate (HR) of the participant and the frames per second or refresh rate of the ultrasound recording (measured in Hz).

$$\# \text{ of frames for baseline} = HR \text{ (bpm)} \times \frac{1\text{min}}{60\text{sec}} \times 15 \text{ cycles} \times \text{refresh rate (Hz)}$$

$$\# \text{ of frames for peak} = HR \text{ (bpm)} \times \frac{1\text{min}}{60\text{sec}} \times 3 \text{ cycles} \times \text{refresh rate (Hz)}$$

Moreover, the measurements extracted from the video clips were calibrated to accurately reflect the actual artery diameter utilizing the ruler tool within the CaroLab software. This involved multiplying the diameter readings for both the popliteal and brachial arteries by a factor obtained through the ruler tool. This adjustment compensated for inaccurate diameter readings that occurred during the transfer of ultrasound clips from the ultrasound to CaroLab. Figure 10 shows CaroLab software analysis of a brachial artery to determine changes in diameter. This includes ruler-determined correction factor, blood vessel wall tracking, refresh rate (Hz), and HR (bpm) all circled in red.

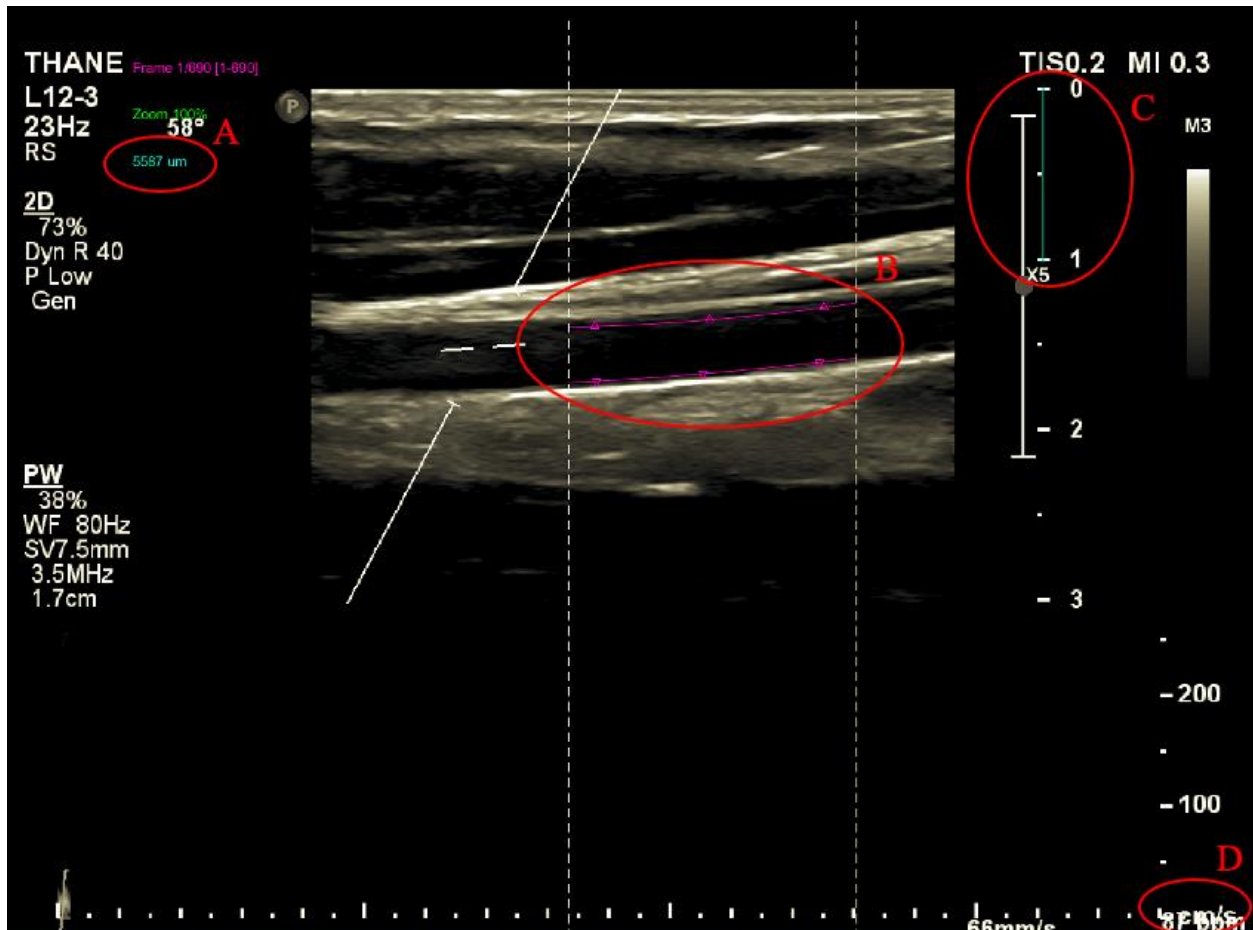


Figure 10. The screenshot of the CaroLab vessel wall tracking software illustrates several key features. Red circles highlight: (A) the conversion factor, (B) vessel wall tracking guide points, (C) the ruler tool used to determine the conversion factor, and (D) the average heart rate in beats per minute over the testing period.

After transferring the diameter readings to Excel, the baseline diameter was determined by averaging the diameter readings over 15 heart cycles. This baseline diameter was then multiplied by the previously determined conversion factor. Next, the peak diameter was calculated by averaging the highest diameter readings over three heart cycles following cuff release. Subsequently, this peak diameter was multiplied by the conversion factor to obtain the true peak vessel diameter. To quantify arterial response to FMD, relative percent dilation was calculated using baseline and peak vessel diameters. These relative percent dilation values were determined for pre- and post-exercise conditions under both control and salt-loaded conditions.

$$\% \text{ difference} = \frac{\text{Peak diameter} - \text{Baseline diameter}}{\text{Baseline diameter}} \times 100$$

Antibody titration

Antibody titrations were conducted to determine the optimal amounts of each type of fluorescent antibody per sample. In five tube arrays, each antibody was distributed in decreasing concentrations into the tubes which contained equal amounts of a lysed and washed human blood. Fluorescence was then measured using the flow cytometer for each tube of the array and the staining index was calculated from the populations of leukocytes stained. Illustrated in Figure 11, the stain index is defined as the ratio of the separation between the positive and negative populations divided by two times the standard deviation (SD) of the negative population (Kalser 2023).

$$\text{Stain Index} = \frac{MFI_{pos} - MFI_{neg}}{2 \times SD_{neg}}$$

The stain index was calculated for each volume of antibody used in the six tube arrays, ranging from 0.25 μL to 5 μL . It was determined that 2.5 μL was the optimal antibody volume for staining the cell populations of interest. This volume yielded an equivalent stain index value to the BIORAD-recommended 5 μL , indicating optimal staining efficiency. The Cytotflex flow cytometry software provided the mean fluorescence intensity (MFI) and SD required for stain index calculations.

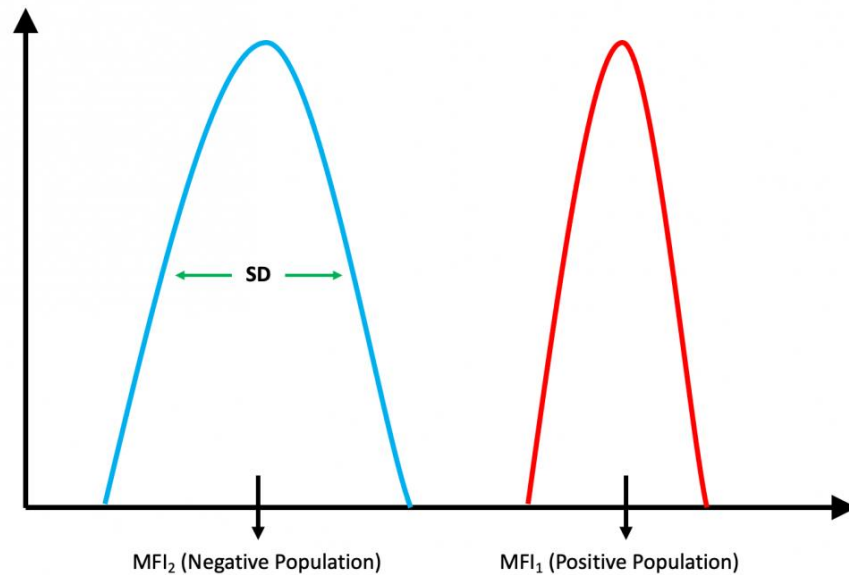


Figure 11. The stain index is the ratio of the separation between the positive population (red) and the negative population (blue), divided by two times the standard deviation of the negative population. MFI is the mean fluorescence intensity for positive and negative populations (Kaiser 2023).

Blood storage and preparation for flow cytometry

Once the participant's blood was drawn in EDTA tubes, the blood was divided into 1 mL and 4 mL aliquots, for flow cytometer leukocyte enumeration and glyocalyx components respectively. Blood leukocyte analysis was conducted immediately to maintain the accuracy of leukocyte counts (Greineder and Younger 2006; Sdek et al. 2020). Blood plasma used to determine glyocalyx components was stored at -80°C for later ELISA screening. A 1 mL aliquot of whole blood was exposed to red blood cell lysis buffer in a 10:1 ratio in a 15 mL centrifuge tube. After the addition of lysis buffer to the blood, it was rocked moderately for 10 minutes. After 10 minutes, or once the sample appeared clear, the sample was centrifuged at 300 g to pellet the peripheral blood mononuclear cells (PBMCs). The lysed RBC layer was discarded. Next, the sample was washed to remove cell fragments and residual plasma using 5 mL of fluorescence-

activated cell sorting buffer (FACS). For the wash step, the pellet was resuspended in 5 mL of FACS, transferred to a 5 mL FACS tube, centrifuged, and the supernatant removed. Post-wash, the pellet was resuspended again in 100 μ L of FACS and treated with 5 μ L of Fc receptor blocker. The sample was incubated for 20 minutes at room temperature. Next, the sample was stained with the designated antibodies to identify populations of leukocytes, neutrophils, monocytes, and NK cells. Table 1 represents the markers and fluorophores selected to observe the immune cell populations of interest.

Table 1. Surface markers and fluorophores for immune cells.

Surface Marker	Fluorophore	Excitation (nm)	wavelength	Emission (nm)	wavelength	Immune cell
CD45	FITC	497-499		516-519		Leukocyte
CD14	PacBlue	404-406		454-456		Monocyte
CD56	PE	564-566		575-576		NK cell
CD66b	APC	650-652		659-661		Granulocyte

Note: Wavelength ranges for fluorophores are for 99% excitation and emission and were found using Biolegend's spectra analyzer tool (Biolegend Inc, 2023).

The lysed and washed blood samples were stained by distributing 10 μ L of a master mix of antibodies containing 2.5 μ L of each fluorescent antibody. Stained sample tubes were incubated in the dark for 30 minutes. Samples were then diluted further in FACS buffer to bring the volume to 1 mL. Each sample was then analyzed using a flow cytometer (Cytotflex, Beckman Coulter). Figure 12 provides the general outline of blood preparation for flow cytometry.

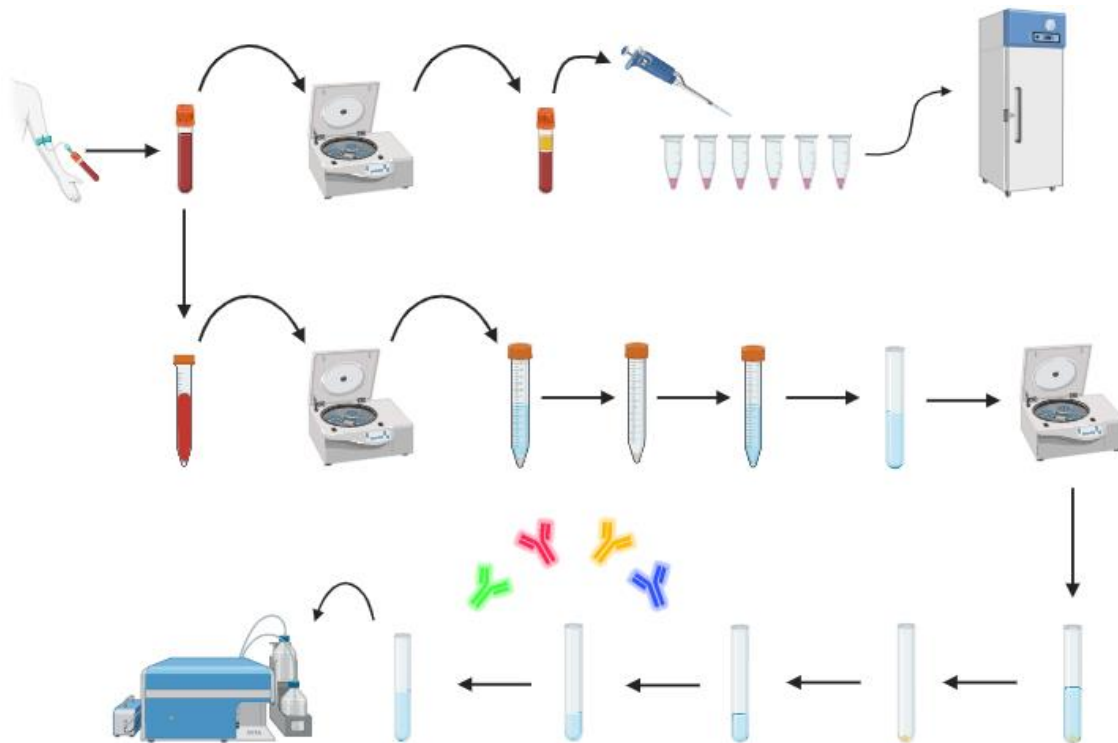


Figure 12. A 1 mL aliquot of whole blood was lysed with red blood cell lysis buffer (10:1 ratio) in a 15 mL centrifuge tube, followed by centrifugation at 300 g to pellet the peripheral blood mononuclear cells (PBMCs). The lysed RBC layer was discarded, and the remaining pellet was washed with 5 mL of fluorescence-activated cell sorting buffer (FACS). After resuspension and incubation with Fc receptor blocker, the sample was stained with designated antibodies to identify leukocyte populations. Stained samples were incubated, resuspended, and analyzed using a flow cytometer (Cytotflex, Beckman Coulter).

Flow cytometry

Before each testing day, the Cytotflex Flow Cytometer was cleaned using the “daily clean” function, which utilizes tubes of cleaning solution and deionized water. The system was then set to the excitation wavelengths of each antibody fluorophore as described in Table 1. Pre- and post-exercise tubes were analyzed. The final volume of each tube was 1 mL to ensure the cell concentrations fell between $1-5 \times 10^6$ cells/ μL . Each tube was set to display a maximum of 100,000 events. The “record” function was used to limit the sample volume to 1 mL, with a sample speed of 60 $\mu\text{L}/\text{minute}$. Following the pre- and post-exercise samples, the backflush function was

employed, and deionized water was run through for 30 seconds to clear any residual sample from the previous tube. After analyzing all tubes, the data was saved onto an external hard drive, and the flow cytometer underwent another "daily clean" function.

Gating strategy

Once the samples were analyzed using the flow cytometer, a series of gating steps were applied to quantify populations of the antibody-labeled immune cells. First, the sample data was separated on a histogram of all events (cells) for CD45⁺ and CD45⁻ populations thereby isolating the general leukocyte cell population and non-leukocytes. The leukocyte population was then plotted on a forward scatter and side scatter plot with forward scatter representing differences in cell size and side scatter representing differences in granularity. This allowed three general leukocyte populations to be identified: granulocytes, lymphocytes, and monocytes. Each population was gated and a histogram representing the fluorescence intensity of events was displayed in separate plots. For example, the granulocyte population was gated and a histogram of the fluorescence intensity of the CD66b antibody marker was displayed. Two distinct peaks could be identified, those that were CD66b⁺ cells and those that did not fluoresce and were considered CD66b⁻ cells. CD66b⁺ cells were recognized as the neutrophil population. The same strategy was used for monocytes and natural killer cells. Using this gating strategy, the flow cytometer program provided population distributions of cells/ μ L and the percent of each population among the entire leukocyte population. The absence of CD45⁻ cells is due to the blood preparation protocol's leukocyte isolation procedure, where RBCs are lysed, and other cell debris is removed through resuspension and centrifugation, resulting in a pellet containing only white blood cells. Regarding the NK cell or CD56⁺ cell population, two peaks are observed, both of which are CD56⁺. One peak

represents CD56⁺ bright cells, while the other represents CD56⁺ dim cells. These bright and dim CD56⁺ NK cells denote two distinct subpopulations of NK cells. However, analyzing these subpopulations was beyond the scope of this study. Figure 13 displays the general outline of gating to find each cell population. Combining this information with the testing timeline enabled us to measure the counts of different immune cell populations before and after subjects underwent a high salt diet, as well as before and after exercise.

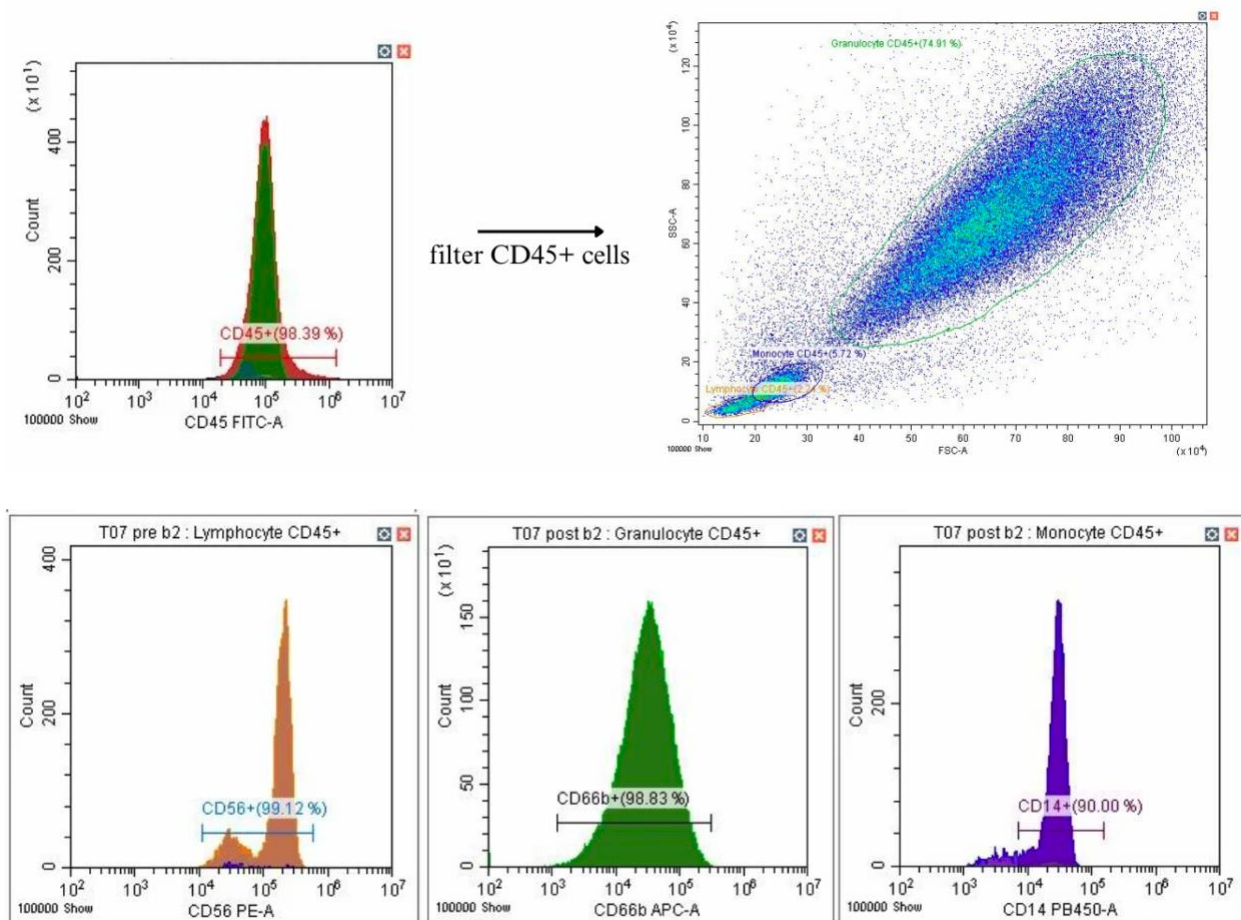


Figure 13. The flow cytometry gating strategy involved enumerating NK cell (CD56⁺), neutrophil (CD66b⁺), and monocyte (CD14⁺) populations. The absence of negative populations for CD45⁺ resulted from the isolation of white blood cells during the blood preparation procedure. Gating for two peaks within the CD56⁺ population was due to the presence of CD56⁺ bright and dim subpopulations, representing distinct subsets of NK cells.

Statistics

Statistics for FMD were performed using JASP (Version 0.17.1) software (JASP Team 2023). A 3-way repeated measure ANOVA was performed on FMD data separating conditions of: pre- and post-exercise, before and after salt, and before and after control. For flow cytometry data analysis, 3-way RM ANOVA was performed for the same repeated measures analyzing cells/ μ L and percent of the total leukocyte population.

RESULTS

Popliteal FMD

Popliteal FMD before and after exercise was the only measure significantly different across all conditions. Table 2 and Figure 14 show that post-exercise popliteal FMD was reduced by 2.7 % (95% CI: 1.8 to 3.5%, $p < 0.01$).

Table 2. Post Hoc comparison of pre- and post-exercise conditions found a significant mean difference (n=4).

		95% CI for Mean Difference					
Mean Difference (%)		Lower	Upper	SE	t	p	
Pre	Post	2.654	1.806	3.502	0.266	9.964	0.002

Note. Results are averaged over the levels of condition and time.

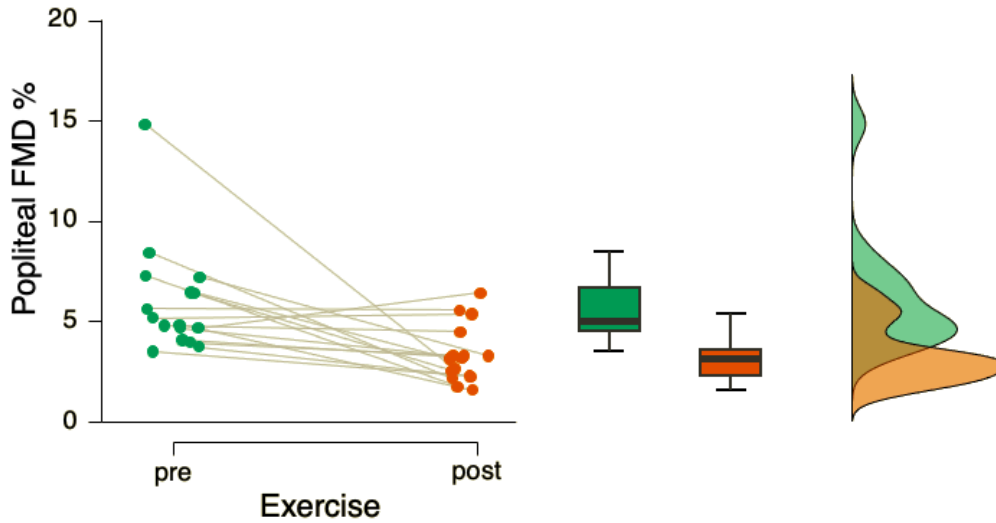


Figure 14. Exercise effects on popliteal artery flow-mediated dilation (n=4). Post-exercise popliteal FMD was reduced by 2.6% (95% CI: 1.8 to 3.5%, $p < 0.01$), as determined by post hoc analysis of exercise condition. Results are averaged over the levels of condition and time (n=4).

For all other comparisons of popliteal FMD, no other relationships such as those between salt and sugar supplementation, showed any significant changes (Appendix 1). This can be seen in Table 3 and Figure 15 which displays the lack of significant differences before and after high salt intake, before and after sugar intake, and between after-salt and after-sugar conditions.

Table 3. Post Hoc comparison of condition and time displaying no significant differences ($p > 0.05$) (n=4).

Condition * Time		Mean Difference	SE	t	p
Salt, Before	Sugar, Before	1.096	0.851	1.288	0.604
	Salt, After	0.614	0.929	0.661	0.908
	Sugar, After	0.575	1.033	0.557	0.941
Sugar, Before	Salt, After	-0.483	1.033	-0.467	0.964
	Sugar, After	-0.521	0.929	-0.561	0.940
Salt, After	Sugar, After	-0.038	0.851	-0.045	1.000

Note. Results are averaged over the levels of: exercise

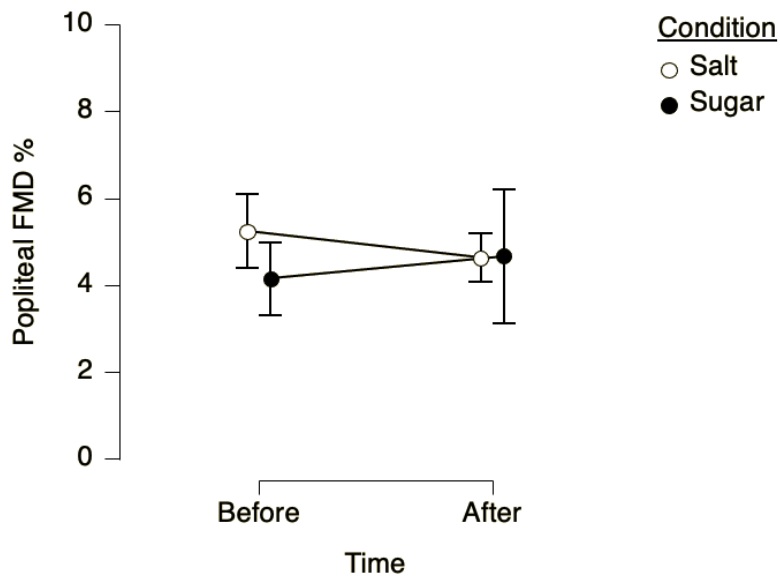


Figure 15. Effects of salt and sugar on popliteal FMD % including standard error bars. Results are averaged over the levels of exercise. None displayed significance ($p>0.05$) ($n=4$).

Mean values for popliteal FMD are reported below (Table 4). In Table 4, the exercise-induced reductions in popliteal FMD are quite pronounced, and there may have been a slight trend in FMD reduction after a high-salt diet, but this was not found to be significant ($p=0.347$) (Appendix 1).

Table 4. Mean percent dilation of the popliteal artery for, condition (salt or sugar), time (before or after), and exercise (pre- and post-exercise) measured through FMD ($n=4$).

Condition	Time	Exercise	N	Mean (%)	SD (%)
Salt	Before	Pre	4	6.195	1.667
		Post	4	4.291	1.963
	After	Pre	4	5.415	1.366
		Post	4	3.843	1.158
Sugar	Before	Pre	4	5.520	1.693
		Post	4	2.774	1.195
	After	Pre	4	6.864	5.341
		Post	4	2.471	0.704

Brachial FMD

Brachial FMD remained unchanged across all conditions, including pre- and post-exercise (Appendix 1). Table 5 displays the mean brachial FMD values for condition (salt or sugar), time (before or after), and exercise (pre- and post-exercise).

Table 5. Mean percent dilation of the brachial artery for, condition (salt or sugar), time (before or after), and exercise (pre- and post-exercise) measured through FMD (n=4).

Condition	Time	Exercise	N	Mean (%)	SD (%)
Salt	Before	Pre	4	6.813	1.579
		Post	4	5.788	1.421
	After	Pre	4	6.597	2.761
		Post	4	5.884	2.207
Sugar	Before	Pre	4	6.548	1.850
		Post	4	6.436	3.375
	After	Pre	4	7.351	1.586
		Post	4	7.726	3.465

Figure 16 also displays the lack of any significant changes in brachial FMD before and after salt treatment, and pre- and post-exercise.

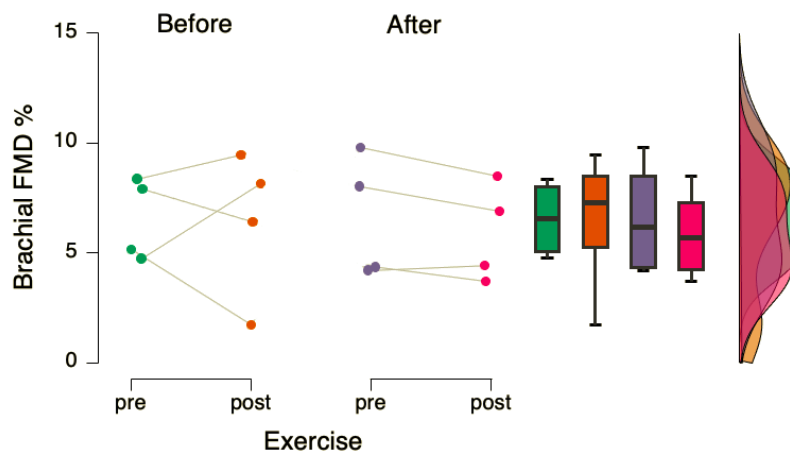


Figure 16. Brachial FMD % before and after a high salt diet and pre- and post-exercise showed no significant differences (n=4).

There was also no change in brachial FMD between salt and sugar conditions (Figure 17). The statistical analysis for all variables for brachial FMD are shown in Appendix 1.

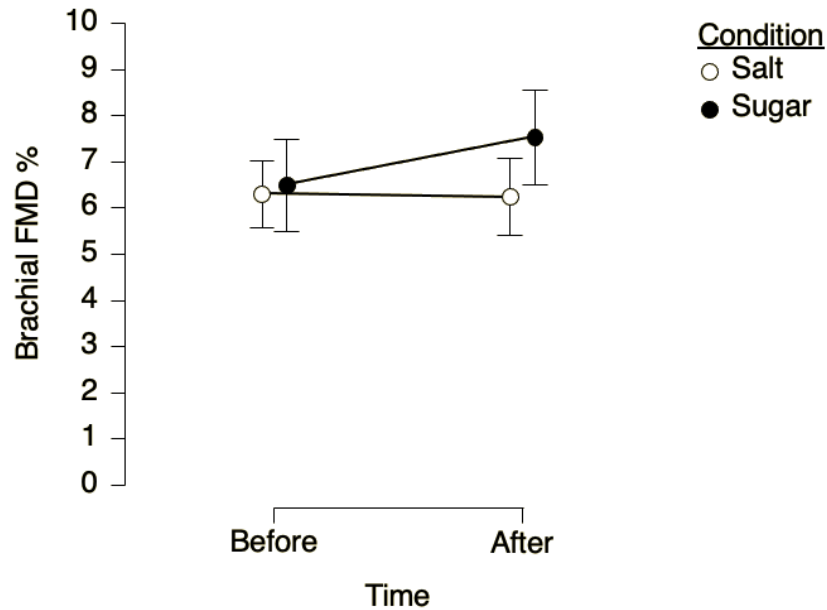


Figure 17. Brachial artery FMD % before and after salt intake and sugar intake. Results are averaged over the levels of exercise (n=4).

Changes in baseline artery diameters

Baseline artery diameter of popliteal and brachial arteries did not change when comparing HSD, control, and pre-treatment conditions (Appendix 1). Table 7 displays the mean baseline diameters for pre- and post-exercise, brachial or popliteal arteries, and conditions of sugar (placebo), baseline (none), or salt (HSD).

Table 6. Baseline artery diameters displayed in μm (n=4).

Exercise	Artery	Condition	N	Mean (μm)	SD (μm)
Pre	Brachial	Sugar	4	3897.750	673.448
		Baseline 1	4	3781.500	391.374
		Salt	4	3744.250	559.170
		Baseline 2	4	3865.500	611.216
	Popliteal	Sugar	4	5487.750	496.161
		Baseline 1	4	5889.000	637.125
		Salt	4	5884.750	523.482
		Baseline 2	4	6039.000	310.680
Post	Brachial	Sugar	4	3877.750	648.529
		Baseline 1	4	3808.750	523.201
		Salt	4	3778.500	666.243
		Baseline 2	4	3935.500	454.006
	Popliteal	Sugar	4	5605.000	170.366
		Baseline 1	4	5555.500	627.608
		Salt	4	5991.250	547.537
		Baseline 2	4	5216.000	1755.325

Flow cytometry of blood leukocyte populations

Blood leukocyte populations generally remained stable across all conditions, with no significant changes ($p > 0.05$) observed in the counts of leukocytes, NK cells, and neutrophils per microliter (Appendix 1). However, monocytes exhibited a mean decrease of 20.17 cells/ μL (95% CI: 2.31 to 38.04 cells/ μL , $p < 0.05$) when comparing before and after salt intake and the control condition (sugar). This difference was identified through data analysis shown in Appendix 1. The percent of the total leukocyte population remained unchanged for all cell types across all conditions (Appendix 1). Tables 6-9 display mean cells/ μL and 10-12 display the mean percent of the total leukocyte population for each analyzed condition.

Table 7. Leukocyte cells/ μL for, condition (salt or sugar), time (before or after), and exercise (pre- and post-exercise) measured through flow cytometry (n=4).

Condition	Time	Exercise	N	Mean (cells/ μL)	SD (cells/ μL)
Sugar	Before	Pre	4	2967	1428
		Post	4	2707	1596
	After	Pre	4	2442	2177
		Post	4	2702	2350
Salt	Before	Pre	4	2827	1700
		Post	4	2358	1919
	After	Pre	4	2292	1441
		Post	4	2404	1454

Table 8. Neutrophil cells/ μL for, condition (salt or sugar), time (before or after), and exercise (pre- and post-exercise) measured through flow cytometry (n=4).

Condition	Time	Exercise	N	Mean (cells/ μL)	SD (cells/ μL)
Sugar	Before	Pre	4	2068	979
		Post	4	1771	995
	After	Pre	4	1615	1409
		Post	4	1971	1959
Salt	Before	Pre	4	1969	1173
		Post	4	1510	1215
	After	Pre	4	1598	1016
		Post	4	1729	1074

Table 9. Monocyte cells/ μL for, condition (salt or sugar), time (before or after), and exercise (pre- and post-exercise) measured through flow cytometry (n=4).

Condition	Time	Exercise	N	Mean (cells/ μL)	SD (cells/ μL)
Sugar	Before	Pre	4	161	110
		Post	4	161	141
	After	Pre	4	130	135
		Post	4	117	125
Salt	Before	Pre	4	157	116
		Post	4	149	154
	After	Pre	4	149	114
		Post	4	152	129

Table 10. NK cells/ μL for, condition (salt or sugar), time (before or after), and exercise (pre- and post-exercise) measured through flow cytometry (n=4).

Condition	Time	Exercise	N	Mean (cells/ μL)	SD (cells/ μL)
Sugar	Before	Pre	4	126	153
		Post	4	141	181
	After	Pre	4	95	125
		Post	4	73	81
Salt	Before	Pre	4	125	154
		Post	4	137	185
	After	Pre	4	111	118
		Post	4	94	85

Table 11. Neutrophil percent of the total leukocyte population for, condition (salt or sugar), time (before or after), and exercise (pre- and post-exercise) measured through flow cytometry (n=4).

Condition	Time	Exercise	N	Mean (%)	SD (%)
Sugar	Before	Pre	4	70.4	4.3
		Post	4	66.4	6.3
	After	Pre	4	65.5	7.9
		Post	4	66.8	15
Salt	Before	Pre	4	71.0	5.0
		Post	4	65.3	4.9
	After	Pre	4	70.5	4.2
		Post	4	71.9	2.6

Table 12. Monocyte percent of the total leukocyte population for, condition (salt or sugar), time (before or after), and exercise (pre- and post-exercise) measured through flow cytometry (n=4).

Condition	Time	Exercise	N	Mean (%)	SD (%)
Sugar	Before	Pre	4	4.8	2.0
		Post	4	4.7	2.2
	After	Pre	4	4.6	3.1
		Post	4	3.9	2.5
Salt	Before	Pre	4	4.7	2.0
		Post	4	4.4	2.5
	After	Pre	4	5.6	2.1
		Post	4	4.9	2.6

Table 13. NK cell percent of the total leukocyte population for, condition (salt or sugar), time (before or after), and exercise (pre- and post-exercise) measured through flow cytometry (n=4).

Condition	Time	Exercise	N	Mean (%)	SD (%)
Sugar	Before	Pre	4	3.3	3.7
		Post	4	4.3	3.9
	After	Pre	4	2.9	3.8
		Post	4	3.0	2.1
Salt	Before	Pre	4	3.3	3.7
		Post	4	4.3	3.9
	After	Pre	4	3.5	3.2
		Post	4	3.3	2.3

Cardiovascular fitness variables

$\dot{V}O_2$ max values were calculated by averaging 30 seconds of $\dot{V}O_2$ breath-by-breath data at peak work rate for each participant (Table 15). The single highest value of oxygen uptake is also included in Table 15 represented by “ $\dot{V}O_2$ peak”. Max heartrate, age, and self-reported extracurricular activities are also included.

Table 14. Cardiovascular fitness variables (n=4).

$\dot{V}O_2$ max (mL/min/kg)	$\dot{V}O_2$ peak (mL/min/kg)	Max HR (bpm)	Age	Reported activities	Sex
28.44	35.07	198	22	Weight training, Soccer	Female
42.39	51.32	198	22	Soccer	Male
48.52	54.24	196	24	Rugby	Male
40.40	44.75	197	23	Weight training, Football	Male

DISCUSSION

The pathways of endothelial dysfunction from high salt intake are complex and involve disruption of various biochemical pathways, alterations in the ESL’s physical properties, and, potentially, changes in immune cell activity and recruitment. To determine the relationships among salt, the ESL, and the immune system, we conducted experiments involving acute bouts of exercise

and after two weeks of high dietary salt intake. This approach allowed us to examine how high salt intake affects the ESL and endothelial function when the glycocalyx is perturbed by exercise-induced shear stress and immune system activation. Through FMD measurements and flow cytometry analysis of specific leukocyte populations, we aimed to study these effects.

Local glycocalyx shedding exerts a greater influence on endothelial dysfunction than the effects of high salt intake

The main finding of this study was that exercise reduced FMD solely in an artery that supplies the exercising limbs, the popliteal artery (a relative decrease of 44%). This finding supports the hypothesis of locally caused endothelial dysfunction from an acute bout of exercise. Our testing also revealed no reduction in FMD responses when comparing pre- and post-exercise measurements of the brachial artery. This suggests that the immediate impact of exercise, particularly concerning the disturbance of NO-mediated dilation, primarily affected the popliteal artery, which supplies blood to locally active skeletal muscles in the legs. There was no change in FMD after the HSD at the popliteal or brachial arteries, suggesting that exercise's acute effects may induce greater reductions than a HSD.

Local dysfunction pathways may involve heightened oxidative stress surrounding the active skeletal muscle and/or damage to the eGC. ROS are generated predominantly by contracting skeletal muscles during physical activity and can increase depending on exercise intensity (He et al. 2016; McArdle et al. 2001; Zuo et al. 2015). These findings mirror the findings of Sakellariou et al. (2013), who reported that exercise can result in a 1–3-fold increase in O_2^- levels in active muscle groups. Potentially, these local increases in ROS could interfere with NO-mediated vasodilation. O_2^- readily binds to NO forming $ONOO^-$. This interaction reduces NO's availability

to promote vasodilation and interferes with eNOS NO production (Janaszak-Jasiecka et al. 2023). Both O_2^- and $ONOO^-$ can oxidize BH_4 , a crucial cofactor in eNOS activity (Milstien and Katusic 1999). This oxidation leads to the production of O_2^- instead of NO, a phenomenon known as eNOS uncoupling (Janaszak-Jasiecka et al. 2023). An imbalance of NO production from the increased uncoupling of eNOS then leads to a depressed vasodilatory response to shear stress, as quantified by FMD techniques (Janaszak-Jasiecka et al. 2023). It was also described by van Golen et al. (2014) that ROS may contribute to endothelial dysfunction by damaging the eGC, which plays a key role in the mechanotransduction of changes in blood flow to cause NO-mediated vasodilation (Pahakis et al. 2007). Many of the proposed pathways of Na^+ -related dysfunction involve causing oxidative stress, from increased NADPH activity and expression, as well as decreased SOD activity and expression (Lenda and Boegehold 2002; Zhu et al. 2007; Kitiyakara 2003; Majerczak et al. 2017; Guers et al. 2019). We suspect that the lack of change in FMD response in both the popliteal and brachial arteries when on a HSD, alongside observing a decrease in the popliteal artery with exercise, could be because salt may not disrupt endothelial function as much as exercise does locally. We also did not find any differences between post-exercise FMD after HSD and after no salt loading. This suggests that the release of Na^+ stored in the ESL due to glycocalyx shedding from exercise may not happen or, if it does, it may not cause significant endothelial dysfunction. Locally influenced dysfunction is further supported by our finding of exercise-induced endothelial dysfunction only in the popliteal artery and not the brachial artery.

The local effects of exercise may have caused greater dysfunction compared to the Na^+ -related pathways of dysfunction and the systemic disruptions to dilation caused by exercise. Bike exercise likely increased mechanical shear stress due to the heightened blood flow to the actively working skeletal muscles in the legs (Sarelius and Pohl 2010). This increase in blood flow in the

legs compared to the arms may have caused greater shear stress and damage to the eGC in the popliteal artery compared to the brachial artery. Additionally, local oxidative stress and exercise by-products could have impaired vasodilation in the popliteal artery more so than the brachial artery (Kröpfl et al. 2021; Nishiyama et al. 2017). The increased temperature of the working muscles during exercise could further exacerbate these effects, leading to a more pronounced suppression of vasodilation in the popliteal artery compared to the brachial artery (Chen et al. 2023). All of the above factors may have culminated in a reduced popliteal FMD after exercise, but not brachial FMD.

It is well understood that the eGC plays a key role in the mechanotransduction of shear stress to stimulate the eNOS/NO/cGMP vasodilatory pathway (Reitsma et al. 2007). We observed that endothelial function was not significantly affected by the HSD we gave our participants. Also, damage to the eGC preventing mechanotransduction may be more detrimental to endothelial function than other pathways involving Na⁺, such as endothelial cell stiffening. Although excess Na⁺ is known to contribute to increased systemic oxidative stress, our finding of unchanged FMD post-HSD but a reduced FMD after exercise may suggest that locally produced ROS from exercise causes a more disruptive increase in oxidative stress than a HSD does systemically. This combination of local oxidative stress and shear stress could cause much greater damage to the eGC and endothelial dysfunction than the systemic effects of a HSD and other Na⁺-related dysfunction pathways.

Kröpfl et al. (2021) and Lee et al. (2019) both found eGC shedding by measuring glycocalyx components in the serum after exercise similar to our exercise bout but did not quantify endothelial dysfunction using FMD pre- and post-exercise. However, Ghiarone et al. (2018) demonstrated when degrading the eGC enzymatically using neuraminidase, FMD was

significantly reduced in rats. Bar et al. (2019) also found that glycocalyx injury coincided with the impairment of endothelium-dependent vasodilation and NO-dependent function. Grandys et al. (2023) also provided support for glycocalyx degradation leading to reductions in FMD, observing a marked decrease in FMD in overtrained female track athletes who had significantly higher serum concentrations of HA and SDC-1, caused by ESL damage. However, this study was focused on the systemic effects of overtraining on endothelial function, not necessarily the direct impact of locally caused glycocalyx damage. Grandys et al. (2023) found correlations between catabolic-anabolic hormone balance changes, eGC damage, and reduced FMD among overtrained athletes, but did not specifically compare brachial and popliteal artery FMD after a bike exercise. Specifically, they looked at intensive periods of exercise training (~13 hours per week) in elite track athletes causing repeated instances of glycocalyx damage without sufficient time for repair. This differed from our stimulus of single bouts of strenuous bike exercise, followed by immediate testing of brachial and popliteal artery FMD. However, they suggested that the overtraining response resembled exercise-induced acute changes in glycocalyx shedding markers. They cited that increased glycocalyx shedding markers resulted from enhanced blood flow, decreased antioxidative capacity, and increased ROS and cytokines.

Further investigation is needed to understand the specific local effects of exercise-induced glycocalyx damage on endothelial dysfunction, particularly concerning FMD responses, as there is limited human research in this area. The relative contributions of shear stress compared to ROS in terms of glycocalyx damage could also be an area of investigation. Future studies are also needed to compare the local and systemic effects of exercise at different intensities and modalities concerning ESL integrity and endothelial dysfunction. This will provide insights into the relative

significance of glycocalyx damage compared to other pathways in post-exercise and post-HSD endothelial dysfunction.

Inflammation response to exercise

Inflammation involves a series of cellular and molecular events that result in increased body temperature, capillary dilation, and the production of soluble components in the blood (Cerqueira et al. 2020). These responses, triggered by stressors and crucial for host defence and tissue homeostasis, help eliminate harmful substances and damaged tissue among other functions (Cerqueira et al. 2020). Acute moderate to high-intensity exercise induces a rise in pro-inflammatory cytokines followed by the release of anti-inflammatory cytokines that attenuate the inflammatory response (Moldoveanu et al. 2001). Common markers of inflammation, such as C-reactive protein (CRP) and TNF- α , have been shown to cause eGC damage and inhibit eNOS activity (Devaraj et al., 2009; Qu et al., 2021). However, it is unlikely these markers were elevated after our prescribed exercise session and probably did not contribute to the observed reduction in popliteal FMD. Although IL-6 is consistently upregulated as a myokine released by working skeletal muscles during exercise, TNF- α and CRP do not show consistent increases in the acute exercise response (Petersen and Pedersen 2005). TNF- α and CRP only significantly increased well after exercise or in response to much higher exercise intensities and durations (Cerqueira et al. 2020; Petersen and Pedersen 2005). The absence of CRP and TNF- α involvement in the inflammation response to exercise is important as many studies that correlate inflammation with glycocalyx damage/endothelial dysfunction focus on the effects of these cytokines specifically (Devaraj et al. 2009; Hu et al. 2021; Qamirani et al. 2005; Sproston and Ashworth 2018; Tarbell and Cancel 2016).

IL-6 is also unlikely to contribute to the exercise-induced dysfunction we observed. Although locally working muscles will secrete IL-6, the effects of this cytokine are dependent on the context of its release (Docherty et al. 2022). Initially thought of as a strictly pro-inflammatory signalling molecule, IL-6 mainly has anti-inflammatory effects during exercise (Docherty et al. 2022). During exercise, IL-6 acts as a hormone-like molecule which mobilizes extracellular substrates and/or augments substrate delivery to working muscle (Petersen and Pedersen 2005). IL-6 also has anti-inflammatory effects. It stimulates the production of anti-inflammatory cytokines interleukin-1 receptor antagonist (IL-1ra) and interleukin-10 (IL-10), inhibits TNF- α , and induces the production of hepatocyte-derived acute-phase proteins, many of which have anti-inflammatory properties (Petersen and Pedersen 2005).

The observation of endothelial dysfunction after exercise in the popliteal artery, but not in the brachial artery, suggests that the systemic inflammatory response was not strong enough or not conducive to causing eGC damage and endothelial dysfunction. This is expected considering the low likelihood that the acute exercise bouts used in our study caused increases in TNF- α and CRP. Additionally, IL-6 locally released in response to exercise confers anti-inflammatory and metabolism-related effects during exercise, unrelated to its pro-inflammatory eGC damaging activity in disease states (Docherty et al. 2022; Nash et al. 2022).

Leukocytosis post-exercise

Leukocytosis is a general increase in circulating white blood cells and is commonly observed post-exercise. As early as 1932, this phenomenon was observed and is a fundamental part of the exercise immune response (Edwards and Wood 1932; Rowbottom and Green 2000; Sand et al. 2013). All major leukocyte subpopulations tend to increase in number during exercise

due to hemodynamic shear stress and/or catecholamines acting on leukocyte β_2 -adrenergic receptors (Peake et al. 2017). From light to severe exercise intensities, all populations of immune cells we analyzed have been shown to increase (Leicht et al. 2017; Tvede et al. 1993). While the combined effects of a HSD and exercise are less understood, our findings of no increase in any leukocyte population post-exercise are likely due to a small sample size with high variation, rather than a physiological lack of immune activation from our exercise bout.

Neutrophils

Of the three leukocyte populations we wished to quantify for their changes pre- and post-exercise and pre- and post-high salt intake, neutrophils were of particular interest. In a study on neutrophils and exercise-induced oxidative stress, Quindry et al. (2003) demonstrated that intense exercise prompts the migration of neutrophils to active skeletal muscles, possibly resulting in heightened oxidative stress. Since endurance exercise performed above VT1 significantly boosts the number of circulating neutrophils, it is conceivable that this neutrophilia can contribute to the oxidative stress seen in the blood during high-intensity exercise (Quindry et al. 2003).

Local neutrophil recruitment begins in response to proteins released from injured muscle, like creatine kinase (CK) and myoglobin (Brancaccio et al. 2010). This triggers the release of cytokines, attracting more neutrophils and macrophages to the damaged area, where they become activated (Lee et al. 2017). Neutrophil activation involves the assembly of NADPH-oxidase, generating ROS and initiating a respiratory burst. These ROS, along with hypochlorous acid (HOCl) produced by myeloperoxidase (MPO) activity, facilitate the phagocytosis of cellular debris (Carrera-Quintanar et al. 2020). Ultimately, this process facilitates the removal of muscle debris and tissue repair (Carrera-Quintanar et al. 2020; Patik et al. 2021). However, transiently, this acute

increase in ROS following exercise could potentially disrupt NO-mediated dilation and cause damage to the eGC, resulting in endothelial dysfunction (Carrera-Quintanar et al. 2020; Patik et al. 2021). Normally, to mitigate non-specific damage caused by the respiratory burst, neutrophils possess an antioxidant system that is activated four to five hours after a bout of exercise (Tauler et al. 2002). We did not see a change in neutrophil counts after exercise. This could have resulted from a discrepancy between other studies concerning exercise modality, time of measurement, or exercise intensity. Our exercise bout of concentric cycling in the heavy exercise domain (above VT1, but below VT2) was also unlikely to cause muscle damage and increase CK production (Ueda et al. 2020). Since muscle damage-induced neutrophil recruitment is unlikely to occur during the exercise bout in our study, it is also unlikely that neutrophils contributed to the locally reduced FMD in the popliteal artery. Supporting this, we found no increase in circulating neutrophils immediately after exercise.

Neutrophilia is suggested to increase depending on the relative exercise intensity (Quindry et al. 2003). Leicht et al. (2017) observed that neutrophilia was indeed blunted in an easy cycling bout and epinephrine concentration was lower than at higher exercise intensities. However, the idea that our exercise intensity was insufficient to invoke any neutrophil response is unlikely. Even in the study by Leicht et al. (2017), easy cycling did increase neutrophil populations, just not to the extent of higher intensities. Earlier work by Tvede et al. (1993) also supported an increase in neutrophils at light, moderate, and severe bike exercise intensities. A more probable explanation for the lack of change found in neutrophils after exercise is an insufficient sample size (n=4) and high variation among samples.

In summary, although we did not find changes in populations of neutrophils after exercise (most likely due to high variation and low sample size) it is unlikely neutrophils contributed to the

local endothelial dysfunction we observed in the popliteal artery due to insufficient muscle damage caused by our exercise bout (Ueda et al. 2020). Future studies analyzing neutrophil responses to exercise and contributions to endothelial dysfunction should include a larger participant pool, monitor CK and other muscle damage markers, and track oxidative stress markers.

A HSD also did not affect counts of neutrophil populations and percentages of leukocytes. Supporting our finding, a study by Yi et al. (2015) which measured leukocyte counts of healthy participants found that neutrophil counts were unchanged across all levels of controlled salt intake ranging from 6 g to 12 g per day. Changes in neutrophil counts are thus unlikely to contribute to endothelial dysfunction during an HSD. However, numerous studies have found that a HSD does have noticeable impacts on various neutrophil functions (Krampert et al. 2021; Li et al. 2022; Mazzitelli et al. 2022; Jobin et al. 2020). In general, HSDs seem to have an immunodepressive effect on neutrophils (Li et al. 2022). Krampert et al. (2021) found that in human neutrophils, ROS production was attenuated as a result of a HSD, which caused a suppression of neutrophils' antibactericidal activity. Li et al. (2022) outlined the impacts of high salt on neutrophils, including suppressed degranulation and O_2^- production. Besides inhibiting key immune-related functions of neutrophils, interactions with neutrophil ROS production could also modulate their contributions to oxidative stress under HSDs. We did not observe a change in endothelial function from a HSD in our participants. The attenuation of ROS production from neutrophils could have influenced the unchanged FMD responses before and after high salt intake as well as the lack of brachial artery dysfunction resulting from systemic post-exercise effects.

Neutrophil activity during and after exercise, as well as before and after a HSD, may play a role in regulating oxidative stress, requiring further investigation (Carrera-Quintanar et al. 2020). To better understand the effects of salt intake and exercise on endothelial function and the ESL,

ROS levels before and after a HSD and exercise should be monitored. This, along with studying serum glycocalyx components affected by ESL damage and examining FMD responses, could offer valuable insights into the impact of neutrophils and exercise-induced immune system activation on vascular health and ESL integrity.

Monocytes and macrophages

Macrophages and monocytes are versatile immune cells crucial for various physiological and pathological processes (Kloc and Kubiak 2022). They participate in phagocytosis, and antigen presentation to T cells, and initiate adaptive immune responses essential for immune surveillance and specific immune responses against pathogens. Both monocytes and macrophages secrete cytokines such as TNF- α and interleukins, which regulate inflammation, immune responses, and tissue repair (Austermann et al. 2022). Moreover, macrophages and monocytes modulate immune responses by interacting with other immune cells, exhibiting both pro-inflammatory and anti-inflammatory activities depending on the context (Kloc and Kubiak 2022). Furthermore, monocytes differentiate into tissue-resident macrophages, which have specialized functions tailored to their specific tissue environments, including the removal of excess Na⁺ from the skin (Kloc and Kubiak 2022; Olde Engberink et al. 2019).

In our study, although we found a significant difference for the time condition, this meant that the difference was before and after HSD and the placebo condition. This was most likely a consequence of a relatively small sample size and a high coefficient of variation among participants, not a depressive effect of both high salt intake and slightly increased sugar intake. Although several studies have noted changes in circulating monocytes from high-sugar diets, the supplementation of ~13.8 g of sugar per day over two weeks did not match the levels used in those

studies (Ma et al. 2022). Other studies also found different effects of salt. Contrary to our findings of a mean decrease in monocytes, Yi et al. (2015) reported that a HSD of 12 g per day led to a significantly higher number of immune cell monocytes compared to the same subjects on a lower-salt diet. Additionally, a correlation test by Yi et al. (2015) revealed a strong positive association between salt intake levels and monocyte numbers. Wenstedt et al. (2019) similarly observed that a HSD tended to increase the total number of circulating monocytes. Our study did not observe any reduction in FMD following a HSD in both brachial and popliteal arteries, suggesting that the HSD did not induce a shift in monocyte recruitment leading to endothelial dysfunction.

Other studies have shown that high salt intake can modulate monocyte activity, potentially influencing endothelial function. Wenstedt et al. (2019) found that a HSD shifted monocytes towards a pro-inflammatory phenotype, with higher CCR2 expression and increased IL-6 and MCP-1 secretion. This led to a higher density of macrophages in the skin, possibly contributing to endothelial dysfunction through greater activation and ROS production. Generally, a HSD can increase circulating monocytes in mice and humans, as well as induce pro-inflammatory human monocytes. However, we did not observe this increase after a HSD. Thus, any influence of monocytes and macrophages on endothelial function after high salt intake is likely due to a change in function and retention in the skin rather than an increase in their number in circulation.

The lack of increase in circulating monocytes from concentric cycling at the intensity and duration of our study is not unfounded. In a study by Tvede et al. (1993) that tested the effects of different exercise intensities on leukocyte populations, it was found that a low- and moderate-intensity bike exercise did not cause an immediate increase in monocytes post-exercise. Instead, monocyte levels either increased one to two hours after exercise cessation (Tvede et al. 1993). These findings further support the idea that exercise-induced increases in circulating monocyte

populations likely do not contribute to pathways causing endothelial dysfunction. Additionally, in the context of systemic versus local differences in endothelial dysfunction after exercise, systemic monocyte-related pathways of dysfunction were likely not present, since brachial FMD remained unchanged after exercise and after HSD.

Strenuous exercise can cause a significant increase in circulating leukocytes, including monocytes (Peake et al. 2017). These cells are believed to migrate partly from the marginal pool of the bloodstream, which contains cells loosely adhered to or rolling on vascular endothelium. The recruitment of these cells into the bloodstream is attributed to shear stress and may be mediated by catecholamines (Peake et al. 2017). Strenuous exercise can cause muscle injuries, activating neutrophils and macrophages through interferon- γ (IFN- γ), interleukin-1 (IL-1), and tumour necrosis factor (TNF) (Steinbacher and Eckl 2015). These activated immune cells then produce excessive ROS leading to endothelial dysfunction (Steinbacher and Eckl 2015). However, our exercise bouts were unlikely to trigger these pathways, represented by the lack of increase found in monocytes immediately post-exercise. Muscle damage is more likely to occur during eccentric exercise as opposed to concentric bike exercise, especially at moderate to heavy intensities and relatively short durations (Ueda et al. 2020). Since our bike exercise involved 45 minutes of concentric cycling in the heavy exercise domain, it is unlikely that monocyte recruitment and activation through muscle damage-related pathways occurred.

This lack of local recruitment of ROS-producing immune cells and lack of systemic increases of monocyte populations immediately post-exercise suggests that the exercise immune response in terms of monocyte recruitment is unlikely to contribute to the endothelial dysfunction we observed and immediately post-exercise. Further, while exercise at high intensity and duration may influence function and cause migration to damaged muscle tissue (Peake et al. 2017), our

exercise bout of 45 minutes of heavy-intensity concentric biking is unlikely to result in extensive muscle damage (Ueda et al. 2020).

Several studies have effectively observed the inflammatory and anti-inflammatory phenotypes of macrophages and monocytes using flow cytometry with expanded antibody panels (Austermann et al. 2022; Wonner et al. 2016; Wenstedt et al. 2019). These techniques could serve as valuable guidelines for future research investigating the impact of both exercise and high salt intake on the roles of monocytes and macrophages in vascular damage. Additionally, observing the contribution of ROS by monocytes and macrophages under exercise and HSD conditions may also be useful to shed light on the relative contributions (or lack of) for these immune cells concerning endothelial dysfunction.

Natural killer cells

Initially characterized as large granular lymphocytes capable of natural cytotoxicity against tumour cells, NK cells have since been identified as a distinct lymphocyte lineage, possessing both cytotoxic and cytokine-producing effector capabilities (Vivier et al. 2008). While NK cells are crucial for combating viruses, it remains unclear whether a HSD influences the development and functionality of NK cells and if this contributes to ESL damage. Our study did not show significant changes in the absolute count or percentage of NK cells, however, their functions could still impact endothelial dysfunction under a high-HSD and after exercise. Zeng et al. (2020) found that a HSD in mice decreased NK cell counts in the spleen and lungs and increased ROS levels due to higher NADPH-oxidase subunit expression. Krampert et al. (2021) similarly found that high salt enhanced ROS production in NK cells. This increased ROS production may affect endothelial function by disrupting NO-mediated vasodilation.

Systemic and local inflammatory responses from disease states can cause rapid loss of glycocalyx and its activities, both directly and indirectly (Hu et al. 2021). NK cells contribute to endothelial dysfunction when influenced by high salt intake and exercise. Pro-inflammatory cytokines upregulate enzymes that degrade glycocalyx components (Shamloo et al. 2021). This damage is triggered by TNF- α , bacterial lipopolysaccharides, and other cytokines, promoting the release of metalloproteinases and heparinases (Hu et al. 2021; Tarbell and Cancel 2016). NK cells secrete cytokines such as IFN- γ , TNF- α , and Granulocyte-Macrophage Colony-Stimulating Factor (GM-CSF), contributing to this process (Paul and Lal 2017). Although the inflammation induced by exercise differs from disease-state inflammation, it is unclear whether a HSD, either independently or combined with exercise, may shift the inflammatory response toward glycocalyx damage and endothelial dysfunction or if it has minimal effect on inflammation pathways (Docherty et al. 2022; Petersen and Pedersen 2005; Qu et al. 2021; Sproston and Ashworth 2018).

Although a HSD and exercise can increase NK cell activity and cytokine levels, particularly IFN- γ , which is linked to eGC damage (Rizvi et al. 2021; Quintana-Mendias et al. 2023; Haywood-Watson et al. 2011), we did not observe changes in NK cell counts or FMD after a HSD. This suggests that NK cell contribution to inflammation was not affected by HSD. Exercise reduced popliteal FMD only in the local working muscle, indicating a lack of systemic changes in NK cell function. Future research should focus on specific changes in NK cell activity and function rather than absolute counts and percentages of leukocytes when investigating NK cell influences on endothelial function.

In summary, the investigation into leukocytosis post-exercise sheds light on the web of interactions between exercise-induced immune responses and endothelial function. Leukocyte populations, including neutrophils, monocytes, and NK cells, exhibit diverse responses to exercise

and HSDs and their implications for vascular health remain complex. The mobilization and activation of neutrophils post-exercise may contribute to oxidative stress and potential endothelial dysfunction. However, due to the lack of observed increases in neutrophils and likely insufficient muscle damage caused by our exercise bout, neutrophils are unlikely to contribute to the local popliteal dysfunction post-exercise. Alterations in monocyte populations post-exercise and post-high salt intake likely do not influence inflammation-related pathways or oxidative stress and therefore do not significantly affect endothelial function. Furthermore, the response of NK cells to high salt and exercise may suggest a contribution of immune activation and endothelial dysfunction. However, NK cells were not involved in the local dysfunction in our study and did not cause systemic endothelial dysfunction either. Our findings suggest that the immune response from exercise, given our specific intensity, duration, and modality, is unlikely to contribute to the local or systemic endothelial dysfunction that we observed and is commonly found after exercise. Additionally, a HSD was unlikely to cause a significant enough shift in immune cell function and number to result in systemic disruptions to endothelial dysfunction. Further, if immune system activation is involved, changes in function rather than absolute counts are likely responsible for contributing to endothelial dysfunction. There is a need for further research to determine the precise mechanisms linking exercise, salt intake, and immune responses to endothelial function. Additional studies looking at different oxidative stress markers and alterations in leukocyte function may offer greater insights into preventive strategies and therapeutic interventions for preserving cardiovascular health.

Limitations

There were several limitations to our study. First, we did not control participants' lifestyles during the study period, which could have resulted in variable meals before testing sessions among other influences. We also relied on self-reporting for pill consumption. This metric may not accurately reflect each participant's specific Na⁺ consumption. To verify whether the HSD resulted in higher levels of Na⁺ in our participants compared to when they were on washout and placebo periods, we could use a combination of methods. These methods include 24-hour urine samples, spot urine samples, and more detailed diet tracking or specific diet control. These measures could help ensure a clear distinction between the conditions. Although we did not observe an increase in any immune cell population, a reduction in blood plasma volume can affect hematocrit and leukocyte measurements. Future research should consider this aspect in their analysis for more accurate results.

Menstrual cycles

Another limitation of our study was not tracking the menstrual cycles of female participants. Menstrual hormones influence processes like inflammation and eNOS activity (Reed and Carr 2018; Harris et al. 2022; Chakrabarti et al. 2014). Gaskins et al. (2012) found significant CRP variation across menstrual cycles, with hormone fluctuations affecting inflammation levels (Wander et al. 2008). This could impact endothelial function by influencing inflammation-mediated damage. Specific hormone cycles could also affect endothelial function. For instance, estrogen has been shown to cause NO-dependent vasodilation, which could cause transient increases or reductions to FMD responses through enhanced eNOS activity (Caulin-Glaser et al. 1997; Chambliss et al. 2000). Although our study only included one female participant,

minimizing any effect of menstrual cycles, future research including more female participants should monitor and account for these variations.

Changes to baseline vessel diameter post-exercise

In our study, we observed a decrease in popliteal FMD after exercise. However, it's possible that these reductions are not solely attributed to ROS-mediated disruption, shear-induced shedding of the eGC, or immune response-related factors (Dawson et al. 2013). Dawson et al. (2013) outlined many of the factors that can influence post-exercise FMD measurements, including changes in baseline artery diameter after exercise. Since calculating FMD involves finding the percent difference between baseline and peak artery diameter, the effects of acute exercise on baseline diameter may influence the FMD response. It is possible that alterations in baseline diameter following acute exercise could pose a limitation when using FMD to assess endothelial function immediately post-exercise (Dawson et al. 2013). Larger arteries, like the popliteal artery, tend to exhibit lower FMD. Therefore, a reduction in FMD after exercise might not necessarily indicate a decrease in vascular function itself but rather reflect a diminished dilator reserve, where vasodilation may be challenging in an already dilated or stretched vessel (Gori et al. 2009). However, studies by Birk et al. (2012) and Katayama et al. (2012) demonstrated that even after statistically adjusting for changes in artery diameter, a notable decrease in FMD persisted immediately after exercise. This suggests that alterations in baseline diameter alone do not entirely explain endothelial dysfunction following exercise in all instances. When we examined the initial baseline artery diameters in our study, we did not find any significant differences between the diameters before and after exercise. If future studies with more participants do find significant changes to baseline diameter post-exercise, these changes should be accounted for. Normalization of FMD responses can be achieved through allometric scaling by dividing the peak percentage

change in diameter by the magnitude of the stimulus achieved with reactive hyperemia, represented by shear stress (Pyke and Tschakovsky 2005).

Exercise training inhibits pathways of salt-related dysfunction

Studies have shown decreased FMD and NO production following HSD, but our study found no such effects in either popliteal or brachial arteries. Exercise training may have countered the harmful effects of high salt intake, through variations in participants' pre-study activity levels. Oxidative stress from HSD can disrupt the vasodilatory pathway and damage the ESL. Exercise may mitigate this stress by enhancing antioxidant pathways and reducing vascular damage (Higashi 2015). Enhanced antioxidative pathways from exercise may reduce ROS influence on eNOS uncoupling and eGC damage. Exercise may also protect eGC from ROS-induced damage, preserving shear-induced NO production and Na⁺ buffering capacity. Additionally, exercise may increase glycocalyx thickness, further enhancing Na⁺ buffering (Schmitz et al. 2019; Selvarajah et al. 2017). Participants with exercise training may thus resist oxidative stress from HSD better and maintain endothelial function, explaining our study's findings. Using breath-by-breath data collected from exercise capacity testing, our participants displayed similar $\dot{V}O_2$ max values, and max HR values to active and trained individuals in studies by Kulinski et al. (2014) and Caputo et al. (2003). This suggests that our participant pool could have attained training adaptations prior to participating in our study, giving them greater resistance to the effects of a HSD that otherwise would cause reduced FMD. In addition to breath-by-breath data, our participants reported being involved in regular weight training, and/or participation or past participation in competitive football, rugby, and soccer. Future studies should consider participants' activity levels when investigating HSDs, exercise, and immune response effects on endothelial function.

Dietary contributions to antioxidative capacity

Participants were advised to maintain their normal diets during the study, but we did not specifically control their diets, which could have led to variations in antioxidative capacity. This factor may have contributed to our findings of unchanged endothelial function after a HSD. For instance, a participant with increased consumption of vitamin C or vitamin E may be better equipped to combat oxidative stress factors introduced by the HSD. Greaney et al. (2012) directly determined the effect of antioxidants in restoring redox balance during an HSD, observing that NO-mediated increases in skin blood flow were restored by local infusion of ascorbic acid (vitamin C) in individuals consuming excess Na⁺. In an extensive review of antioxidants and oxidative stress, Tan et al. (2018) concluded that antioxidants can disrupt the spread of free radicals by preventing their formation, thereby reducing oxidative stress. While we do not propose that exercise training or dietary antioxidants could fully eliminate dysfunction caused by these pathways, they may have mitigated the effects to some extent, potentially explaining our observation of unchanged endothelial function after the HSD

CONCLUSIONS

In our study, we found that exercise caused a significant reduction in popliteal FMD, but not brachial FMD after a bout of cycling exercise at one-third work rate between VT1 and VT2. We did not find a reduction in FMD or changes in immune cell populations after a HSD. While unchanging immune cell counts are unexpected, it is unlikely that the exercise immune response is likely to influence endothelial dysfunction. Based on the absence of reduced brachial FMD after exercise and the absence of FMD reduction after high salt intake in popliteal and brachial arteries, we propose that localized effects of exercise caused greater impairment of FMD compared to systemic effects. Increases in blood flow and shear stress in specific active muscles, as well as

local release of ROS, lead to glycocalyx damage and endothelial dysfunction. These localized forces may play a greater role in causing endothelial dysfunction compared to systemic pathways related to oxidative stress, endothelial cell stiffening by high salt, and systemic immune system activation. The bike exercise, targeting skeletal muscles in the leg, likely triggered an influx of blood flow and shear stress, resulting in the shedding of glycocalyx components crucial for NO-mediated dilation. ROS released locally from higher metabolism of active muscles may also have caused glycocalyx damage and reduced NO-bioavailability. Consequently, these factors led to a reduced popliteal artery FMD, but not brachial artery FMD, post-exercise. Our study had several limitations, providing opportunities for future research. More extensive participant tracking of diet, exercise, and menstrual cycles should be incorporated into studies with larger and more diverse participant pools. Additionally, ELISA testing and an expanded panel of antibodies for flow cytometry could help measure glycocalyx components, markers of inflammation and oxidative stress, and immune cell by-products. Such measures could increase our understanding of the intricate yet interconnected roles of salt intake, ESL integrity, and the immune response to exercise, thereby increasing our understanding of endothelial function.

LITERATURE CITED

- Akhtari-Shojaei E. 2011 Jan. Effect of moderate aerobic cycling on some systemic inflammatory markers in healthy active collegiate men. *International Journal of General Medicine*:79. doi:<https://doi.org/10.2147/ijgm.s15065>.
- Anselmi F, Cavigli L, Pagliaro A, Valente S, Valentini F, Cameli M, Focardi M, Mochi N, Dendale P, Hansen D, et al. 2021. The importance of ventilatory thresholds to define aerobic exercise intensity in cardiac patients and healthy subjects. *Scandinavian Journal of Medicine & Science in Sports*. 31(9):1796–1808. doi:<https://doi.org/10.1111/sms.14007>.
- Austermann J, Roth J, Barczyk-Kahlert K. 2022. The Good and the Bad: Monocytes' and Macrophages' Diverse Functions in Inflammation. *Cells*. 11(12):1979. doi:<https://doi.org/10.3390/cells11121979>.
- Balady GJ, Arena R, Sietsema K, Myers J, Coke L, Fletcher GF, Forman D, Franklin B, Guazzi M, Gulati M, et al. 2010. Clinician's Guide to Cardiopulmonary Exercise Testing in Adults. *Circulation*. 122(2):191–225. doi:<https://doi.org/10.1161/cir.0b013e3181e52e69>.
- Bar A, Targosz-Korecka M, Suraj J, Proniewski B, Jaształ A, Marczyk B, Sternak M, Przybyło M, Kurpińska A, Walczak M, et al. 2019. Degradation of Glycocalyx and Multiple Manifestations of Endothelial Dysfunction Coincide in the Early Phase of Endothelial Dysfunction Before Atherosclerotic Plaque Development in Apolipoprotein E/Low-Density Lipoprotein Receptor-Deficient Mice. *Journal of the American Heart Association*. 8(6). doi:<https://doi.org/10.1161/jaha.118.011171>.
- Beaver WL, Wasserman K, Whipp BJ. 1986. A new method for detecting anaerobic threshold by gas exchange. *Journal of Applied Physiology*. 60(6):2020–2027. doi:<https://doi.org/10.1152/jappl.1986.60.6.2020>.
- Birk G, Dawson E, Batterham A, Atkinson G, Cable T, Thijssen DH, Green D. 2012. Effects of Exercise Intensity on Flow Mediated Dilation in Healthy Humans. *International Journal of Sports Medicine*. 34(05):409–414. doi:<https://doi.org/10.1055/s-0032-1323829>. [accessed 2020 Nov 6]. <https://www.dsu.univr.it/documenti/OccorrenzaIns/matdid/matdid013984.pdf>.
- Brancaccio P, Lippi G, Maffulli N. 2010. Biochemical markers of muscular damage. *Clinical Chemistry and Laboratory Medicine*. 48(6). doi:<https://doi.org/10.1515/cclm.2010.179>.
- Bredin SSD, Gledhill N, Jamnik VK, Warburton DER. 2013. PAR-Q+ and ePARmed-X+: new risk stratification and physical activity clearance strategy for physicians and patients alike. *Canadian Family Physician Medecin De Famille Canadien*. 59(3):273–277. <https://pubmed.ncbi.nlm.nih.gov/23486800/>.
- Caputo F, Mello MT, Denadai BS. 2003. Oxygen Uptake Kinetics and Time to Exhaustion in Cycling and Running: a Comparison Between Trained and Untrained Subjects. *Archives of Physiology and Biochemistry*. 111(5):461–466. doi:<https://doi.org/10.3109/13813450312331342337>.

Carrera-Quintanar L, Funes L, Herranz-López M, Martínez-Peinado P, Pascual-García S, Sempere JM, Boix-Castejón M, Córdova A, Pons A, Micol V, et al. 2020. Antioxidant Supplementation Modulates Neutrophil Inflammatory Response to Exercise-Induced Stress. *Antioxidants*. 9(12):1242. doi:<https://doi.org/10.3390/antiox9121242>.

Caulin-Glaser T, García-Cardena G, Sarrel PM, Sessa WC, Bender JR. 1997. 17β -Estradiol Regulation of Human Endothelial Cell Basal Nitric Oxide Release, Independent of Cytosolic Ca^{2+} Mobilization. *Circulation Research*. 81(5):885–892. doi:<https://doi.org/10.1161/01.res.81.5.885>.

CDC. 2024 Jan 17. Leading Causes of Death. Centers for Disease Control and Prevention. <https://www.cdc.gov/nchs/fastats/leading-causes-of-death.htm>.

Cerqueira É, Marinho DA, Neiva HP, Lourenço O. 2020. Inflammatory Effects of High and Moderate Intensity Exercise—A Systematic Review. *Frontiers in Physiology*. 10. doi:<https://doi.org/10.3389/fphys.2019.01550>. <https://www.ncbi.nlm.nih.gov/pmc/articles/PMC6962351/>.

Chakrabarti S, Morton JS, Davidge ST. 2014. Mechanisms of Estrogen Effects on the Endothelium: An Overview. *Canadian Journal of Cardiology*. 30(7):705–712. doi:<https://doi.org/10.1016/j.cjca.2013.08.006>.

Chambliss KL, Yuhanna IS, Mineo C, Liu P, German Z, Sherman TS, Mendelsohn ME, Anderson RGW, Shaul PW. 2000. Estrogen Receptor α and Endothelial Nitric Oxide Synthase Are Organized Into a Functional Signaling Module in Caveolae. *Circulation Research*. 87(11). doi:<https://doi.org/10.1161/01.res.87.11.e44>.

Chen J, Ding C, Cao J, Tong H, Chen Y. 2023. Heat stress combined with lipopolysaccharide induces pulmonary microvascular endothelial cell glycocalyx inflammatory damage in vitro. *Immunity, inflammation and disease*. 11(10). doi:<https://doi.org/10.1002/iid3.1034>.

Cosgun ZC, Fels B, Kusche-Vihrog K. 2020. Nanomechanics of the Endothelial Glycocalyx. *American Journal of Pathology*. 190(4):732–741. doi:<https://doi.org/10.1016/j.ajpath.2019.07.021>.

da Silva GM, da Silva MC, Nascimento DVG, Lima Silva EM, Gouvêa FFF, de França Lopes LG, Araújo AV, Ferraz Pereira KN, de Queiroz TM. 2021. Nitric Oxide as a Central Molecule in Hypertension: Focus on the Vasorelaxant Activity of New Nitric Oxide Donors. *Biology*. 10(10):1041. doi:<https://doi.org/10.3390/biology10101041>. <https://www.mdpi.com/2079-7737/10/10/1041>.

Davis JA, Vodak P, Wilmore JH, Vodak J, Kurtz P. 1976. Anaerobic threshold and maximal aerobic power for three modes of exercise. *Journal of Applied Physiology*. 41(4):544–550. doi:<https://doi.org/10.1152/jappl.1976.41.4.544>.

Dawson EA, Green DJ, Timothy Cable N, Thijssen DHJ. 2013. Effects of acute exercise on flow-mediated dilatation in healthy humans. *Journal of Applied Physiology*. 115(11):1589–1598. doi:<https://doi.org/10.1152/japplphysiol.00450.2013>.

Devaraj S, Yun J-M ., Adamson G, Galvez J, Jialal I. 2009. C-reactive protein impairs the endothelial glycocalyx resulting in endothelial dysfunction. *Cardiovascular Research*. 84(3):479–484. doi:<https://doi.org/10.1093/cvr/cvp249>.

Djrbal L, Lortat-Jacob H, Kwok J. 2017. Chondroitin sulfates and their binding molecules in the central nervous system. *Glycoconjugate Journal*. 34(3):363–376. doi:<https://doi.org/10.1007/s10719-017-9761-z>.

Docherty S, Harley R, McAuley JJ, Crowe LAN, Pedret C, Kirwan PD, Siebert S, Millar NL. 2022. The effect of exercise on cytokines: implications for musculoskeletal health: a narrative review. *BMC Sports Science, Medicine and Rehabilitation*. 14(1). doi:<https://doi.org/10.1186/s13102-022-00397-2>.
<https://bmcsportsscimedrehabil.biomedcentral.com/articles/10.1186/s13102-022-00397-2>.

Dragovich MA, Chester D, Fu BM, Wu C, Xu Y, Goligorsky MS, Zhang XF. 2016. Mechanotransduction of the endothelial glycocalyx mediates nitric oxide production through activation of TRP channels. *American Journal of Physiology-Cell Physiology*. 311(6):C846–C853. doi:<https://doi.org/10.1152/ajpcell.00288.2015>.

Edwards HT, Wood WB. 1932. A study of leukocytosis in exercise. *Arbeitsphysiologie*. 6(1-2):73–83. doi:<https://doi.org/10.1007/bf02009854>.

Florian JA, Kosky JR, Ainslie K, Pang Z, Dull RO, Tarbell JM. 2003. Heparan sulfate proteoglycan is a mechanosensor on endothelial cells. *Circulation research*. 93(10):e136-42. doi:<https://doi.org/10.1161/01.RES.0000101744.47866.D5>. [accessed 2019 Dec 9].
<https://www.ncbi.nlm.nih.gov/pubmed/14563712>.

Foote CA, Ramirez-Perez FI, Smith JA, Thaysa Ghiarone, Morales-Quinones M, McMillan NJ, Augenreich MA, Power G, Burr K, Annayya Aroor, et al. 2023. Neuraminidase inhibition improves endothelial function in diabetic mice. *American Journal of Physiology-heart and Circulatory Physiology*. 325(6):H1337–H1353. doi:<https://doi.org/10.1152/ajpheart.00337.2023>.

Förstermann U, Sessa WC. 2012. Nitric oxide synthases: regulation and function. *European heart journal*. 33(7):829–37, 837a837d. doi:<https://doi.org/10.1093/eurheartj/ehr304>.

Gallo G, Volpe M, Savoia C. 2022. Endothelial Dysfunction in Hypertension: Current Concepts and Clinical Implications. *Frontiers in Medicine*. 8(1). doi:<https://doi.org/10.3389/fmed.2021.798958>.

Gaskins AJ, Wilchesky M, Mumford SL, Whitcomb BW, Browne RW, Wactawski-Wende J, Perkins NJ, Schisterman EF. 2012. Endogenous Reproductive Hormones and C-reactive Protein Across the Menstrual Cycle: The BioCycle Study. *American Journal of Epidemiology*. 175(5):423–431. doi:<https://doi.org/10.1093/aje/kwr343>.

Ghiarone T, Foote CA, Padilla J, Martinez-Lemus LA. 2018. Glycocalyx degradation impairs endothelial function in cultured cells and a mouse model of type 2 diabetes. *The Federation of American Societies for Experimental Biology*. 32(S1). doi:https://doi.org/10.1096/fasebj.2018.32.1_supplement.lb275.

- Gori T, Grotti S, Dragoni S, Lisi M, Di Stolfo G, Sonnati S, Fineschi M, Parker JD. 2009. Assessment of vascular function: flow-mediated constriction complements the information of flow-mediated dilatation. *Heart*. 96(2):141–147. doi:<https://doi.org/10.1136/hrt.2009.167213>.
- Grandys M, Majerczak J, Marzena Frołow, Chłopicki S, Zoladz JA. 2023. Training-induced impairment of endothelial function in track and field female athletes. *Scientific Reports*. 13(1). doi:<https://doi.org/10.1038/s41598-023-30165-2>.
- Greaney JL, DuPont JJ, Lennon-Edwards SL, Sanders PW, Edwards DG, Farquhar WB. 2012. Dietary sodium loading impairs microvascular function independent of blood pressure in humans: role of oxidative stress. *The Journal of Physiology*. 590(21):5519–5528. doi:<https://doi.org/10.1113/jphysiol.2012.236992>.
- Greineder C, Younger J. 2006. Apoptosis of leukocytes over time under various storage conditions. *Shock*. 25(6):51. [accessed 2024 May 3]. https://journals.lww.com/shockjournal/fulltext/2006/06001/apoptosis_of_leukocytes_over_time_under_various.156.aspx.
- Guers JJ, Kasecky-Lardner L, Farquhar WB, Edwards DG, Lennon SL. 2019. Voluntary wheel running prevents salt-induced endothelial dysfunction: role of oxidative stress. *Journal of Applied Physiology*. 126(2):502–510. doi:<https://doi.org/10.1152/jappphysiol.00421.2018>.
- Hadi HAR, Carr CS, Al Suwaidi J. 2005. Endothelial dysfunction: cardiovascular risk factors, therapy, and outcome. *Vascular health and risk management*. 1(3):183–98. <https://www.ncbi.nlm.nih.gov/pmc/articles/PMC1993955/>.
- Hahn RG, Patel V, Dull RO. 2021. Human glycocalyx shedding: Systematic review and critical appraisal. *Acta Anaesthesiologica Scandinavica*. 65(5):590–606. doi:<https://doi.org/10.1111/aas.13797>.
- Harris BS, Steiner AZ, Faurot KR, Long A, Jukic AM. 2022. Systemic Inflammation and Menstrual Cycle Length in a Prospective Cohort Study. *American Journal of Obstetrics and Gynecology*. 228(2). doi:<https://doi.org/10.1016/j.ajog.2022.10.008>.
- Haywood-Watson RJ, Holcomb JB, Gonzalez EA, Peng Z, Pati S, Park PW, Wang W, Zaske AM, Menge T, Kozar RA. 2011. Modulation of Syndecan-1 Shedding after Hemorrhagic Shock and Resuscitation. McNeil P, editor. *PLoS ONE*. 6(8):e23530. doi:<https://doi.org/10.1371/journal.pone.0023530>.
- He F, Li J, Liu Z, Chuang C-C, Yang W, Zuo L. 2016. Redox Mechanism of Reactive Oxygen Species in Exercise. *Frontiers in Physiology*. 7. doi:<https://doi.org/10.3389/fphys.2016.00486>.
- Higashi Y. 2015. Exercise is a double-edged sword for endothelial function. *Hypertension Research*. 39(2):61–63. doi:<https://doi.org/10.1038/hr.2015.127>.
- Hu Z, Cano I, D'Amore PA. 2021. Update on the Role of the Endothelial Glycocalyx in Angiogenesis and Vascular Inflammation. *Frontiers in Cell and Developmental Biology*. 9. doi:<https://doi.org/10.3389/fcell.2021.734276>.

- Jablonski KL, Racine ML, Geolfos CJ, Gates PE, Chonchol M, McQueen MB, Seals DR. 2013. Dietary Sodium Restriction Reverses Vascular Endothelial Dysfunction in Middle-Aged/Older Adults With Moderately Elevated Systolic Blood Pressure. *Journal of the American College of Cardiology*. 61(3):335–343. doi:<https://doi.org/10.1016/j.jacc.2012.09.010>.
- Janaszak-Jasiecka A, Agata Płoska, Wierońska JM, Dobrucki LW, Kalinowski L. 2023. Endothelial dysfunction due to eNOS uncoupling: molecular mechanisms as potential therapeutic targets. *PubMed Central*. 28(1). doi:<https://doi.org/10.1186/s11658-023-00423-2>.
- Widmer R, Lerman A. 2014. Endothelial dysfunction and cardiovascular disease. *Global Cardiology Science and Practice*. 2014(3):43. doi:<https://doi.org/10.5339/gcsp.2014.43>.
- Jobin K, Stumpf NE, Schwab S, Eichler M, Neubert P, Rauh M, Adamowski M, Babyak O, Hinze D, Sivalingam S, et al. 2020. A high-salt diet compromises antibacterial neutrophil responses through hormonal perturbation. *Science Translational Medicine*. 12(536):eaay3850. doi:<https://doi.org/10.1126/scitranslmed.aay3850>. <https://pubmed.ncbi.nlm.nih.gov/32213629>.
- Kakutani N, Fukushima A, Yokota T, Katayama T, Nambu H, Shirakawa R, Maekawa S, Abe T, Takada S, Furihata T, et al. 2018. Impact of High Respiratory Exchange Ratio During Submaximal Exercise on Adverse Clinical Outcome in Heart Failure. *Circulation Journal*. 82(11):2753–2760. doi:<https://doi.org/10.1253/circj.cj-18-0103>.
- Kalser S. 2023 May 31. Stain Index for Flow Cytometry - Explained. *FluoroFinder*. [accessed 2024 May 3]. <https://fluorofinder.com/stain-index-flow-cytometry/#:~:text=The%20stain%20index%20is%20defined>.
- Katayama K, Fujita O, Motoyuki Iemitsu, Kawano H, Iwamoto E, Saito M, Ishida K. 2012. The effect of acute exercise in hypoxia on flow-mediated vasodilation. *European Journal of Applied Physiology*. 113(2):349–357. doi:<https://doi.org/10.1007/s00421-012-2442-5>.
- Kitiyakara C. 2003. Salt Intake, Oxidative Stress, and Renal Expression of NADPH Oxidase and Superoxide Dismutase. *Journal of the American Society of Nephrology*. 14(11):2775–2782. doi:<https://doi.org/10.1097/01.asn.0000092145.90389.65>.
- Kloc M, Kubiak JZ. 2022. Monocyte and Macrophage Function Diversity. *International Journal of Molecular Sciences*. 23(20):12404. doi:<https://doi.org/10.3390/ijms232012404>.
- Korte S, Wiesinger A, Straeter AS, Peters W, Oberleithner H, Kusche-Vihrog K. 2011. Firewall function of the endothelial glycocalyx in the regulation of sodium homeostasis. *Pflügers Archiv - European Journal of Physiology*. 463(2):269–278. doi:<https://doi.org/10.1007/s00424-011-1038-y>.
- Krampert L, Bauer K, Ebner S, Neubert P, Ossner T, Weigert A, Schatz V, Toelge M, Schröder A, Herrmann M, et al. 2021. High Na⁺ Environments Impair Phagocyte Oxidase-Dependent Antibacterial Activity of Neutrophils. *Frontiers in Immunology*. 12:712948. doi:<https://doi.org/10.3389/fimmu.2021.712948>. [accessed 2024 Apr 30]. <https://pubmed.ncbi.nlm.nih.gov/34566968/>.

Kröpfl JM, Beltrami FG, Rehm M, Gruber H-J, Stelzer I, Spengler CM. 2021. Acute exercise-induced glycocalyx shedding does not differ between exercise modalities, but is associated with total antioxidative capacity. *Journal of Science and Medicine in Sport*. 24(7):689–695. doi:<https://doi.org/10.1016/j.jsams.2021.01.010>. [accessed 2024 May 3]. <https://pubmed.ncbi.nlm.nih.gov/33632661/>.

Kulinski JP, Khera A, Ayers CR, Das SR, de Lemos JA, Blair SN, Berry JD. 2014. Association Between Cardiorespiratory Fitness and Accelerometer-Derived Physical Activity and Sedentary Time in the General Population. *Mayo Clinic Proceedings*. 89(8):1063–1071. doi:<https://doi.org/10.1016/j.mayocp.2014.04.019>.

Landmesser U, Harrison DG, Drexler H. 2005. Oxidant stress—a major cause of reduced endothelial nitric oxide availability in cardiovascular disease. *European Journal of Clinical Pharmacology*. 62(S1):13–19. doi:<https://doi.org/10.1007/s00228-005-0012-z>.

Lee EC, Fragala MS, Kavouras SA, Queen RM, Pryor JL, Casa DJ. 2017. Biomarkers in Sports and Exercise: Tracking Health, Performance, and Recovery in Athletes. *Journal of strength and conditioning research*. 31(10):2920–2937. doi:<https://doi.org/10.1519/JSC.0000000000002122>. <https://www.ncbi.nlm.nih.gov/pubmed/28737585>.

Lee S, Kolset SO, Birkeland KI, Drevon CA, Reine TM. 2019. Acute exercise increases syndecan-1 and -4 serum concentrations. *Glycoconjugate Journal*. 36(2):113–125. doi:<https://doi.org/10.1007/s10719-019-09869-z>. [accessed 2024 Apr 30]. <https://pubmed.ncbi.nlm.nih.gov/30949875/>.

Leicht CA, Goosey-Tolfrey VL, Bishop NC. 2017. Comparable Neutrophil Responses for Arm and Intensity-matched Leg Exercise. *Medicine & Science in Sports & Exercise*. 49(8):1716–1723. doi:<https://doi.org/10.1249/mss.0000000000001258>.

Lenda DM, Boegehold MA. 2002. Effect of a high-salt diet on oxidant enzyme activity in skeletal muscle microcirculation. *American Journal of Physiology Heart and Circulatory Physiology*. 282(2):H395–402. doi:<https://doi.org/10.1152/ajpheart.0354.2001>. <https://pubmed.ncbi.nlm.nih.gov/11788385/>.

Lenda DM, Sauls BA, Boegehold MA. 2000. Reactive oxygen species may contribute to reduced endothelium-dependent dilation in rats fed high salt. *American Journal of Physiology-Heart and Circulatory Physiology*. 279(1):H7–H14. doi:<https://doi.org/10.1152/ajpheart.2000.279.1.h7>.

Li X, Alu A, Wei Y, Wei X, Luo M. 2022. The modulatory effect of high salt on immune cells and related diseases. *Cell Proliferation*. 55(9). doi:<https://doi.org/10.1111/cpr.13250>.

Ma X, Nan F, Liang H, Shu P, Fan X, Song X, Hou Y, Zhang D. 2022. Excessive intake of sugar: An accomplice of inflammation. *Frontiers in Immunology*. 13(13). doi:<https://doi.org/10.3389/fimmu.2022.988481>. <https://www.ncbi.nlm.nih.gov/pmc/articles/PMC9471313/>.

Majerczak J, Grandys M, Duda K, Zakrzewska A, Balcerczyk A, Kolodziejcki L, Szymoniak-Chochol D, Smolenski RT, Bartosz G, Chlopicki S, et al. 2017. Moderate-intensity endurance

training improves endothelial glycocalyx layer integrity in healthy young men. *Experimental Physiology*. 102(1):70–85. doi:<https://doi.org/10.1113/ep085887>.

Martini AD, Dalleck LC, Mejuto G, Larwood T, Weatherwax RM, Ramos JS. 2022. Changes in the Second Ventilatory Threshold Following Individualised versus Standardised Exercise Prescription among Physically Inactive Adults: A Randomised Trial. *International Journal of Environmental Research and Public Health*. 19(7):3962. doi:<https://doi.org/10.3390/ijerph19073962>.

Mazzitelli I, Bleichmar L, Melucci C, Gerber PP, Toscanini A, Cuestas ML, Diaz FE, Geffner J. 2022. High Salt Induces a Delayed Activation of Human Neutrophils. *Frontiers in Immunology*. 13. doi:<https://doi.org/10.3389/fimmu.2022.831844>. [accessed 2023 May 8]. <https://doi.org/10.3389%2Ffimmu.2022.831844>.

McArdle A, Pattwell D, Vasilaki A, Griffiths RD, Jackson MJ. 2001. Contractile activity-induced oxidative stress: cellular origin and adaptive responses. *American Journal of Physiology-Cell Physiology*. 280(3):C621–C627. doi:<https://doi.org/10.1152/ajpcell.2001.280.3.c621>.

Microsoft Corporation. 2016. Microsoft Excel. Retrieved from <https://office.microsoft.com/excel>
Milstien S, Katusic ZS. 1999. Oxidation of Tetrahydrobiopterin by Peroxynitrite: Implications for Vascular Endothelial Function. *Biochemical and Biophysical Research Communications*. 263(3):681–684. doi:<https://doi.org/10.1006/bbrc.1999.1422>.

Milusev A, Rieben R, Sorvillo N. 2022. The Endothelial Glycocalyx: A Possible Therapeutic Target in Cardiovascular Disorders. *Frontiers in Cardiovascular Medicine*. 9. doi:<https://doi.org/10.3389/fcvm.2022.897087>.

Moldoveanu AI, Shephard RJ, Shek PN. 2001. The Cytokine Response to Physical Activity and Training. *Sports Medicine*. 31(2):115–144. doi:<https://doi.org/10.2165/00007256-200131020-00004>.

Nash D, Hughes MG, Butcher L, Aicheler R, Smith P, Cullen T, Webb R. 2022. IL-6 signaling in acute exercise and chronic training: Potential consequences for health and athletic performance. *Scandinavian Journal of Medicine & Science in Sports*. 33(1). doi:<https://doi.org/10.1111/sms.14241>.

Nieman DC, Wentz LM. 2019. The compelling link between physical activity and the body's defense system. *Journal of Sport and Health Science*. 8(3):201–217. doi:<https://doi.org/10.1016/j.jshs.2018.09.009>.

Nishiyama SK, Zhao J, Wray DW, Richardson RS. 2017. Vascular function and endothelin-1: tipping the balance between vasodilation and vasoconstriction. *Journal of Applied Physiology*. 122(2):354–360. doi:<https://doi.org/10.1152/jappphysiol.00772.2016>. [accessed 2022 Jan 12]. <https://www.ncbi.nlm.nih.gov/pmc/articles/PMC5338602/>.

Oberleithner H, Peters W, Kusche-Vihrog K, Korte S, Schillers H, Kliche K, Oberleithner K. 2011. Salt overload damages the glycocalyx sodium barrier of vascular endothelium. *Pflügers Archiv* -

European Journal of Physiology. 462(4):519–528. doi:<https://doi.org/10.1007/s00424-011-0999-1>.

Oberleithner H, Riethmüller C, Schillers H, MacGregor GA, de Wardener HE, Hausberg M. 2007. Plasma sodium stiffens vascular endothelium and reduces nitric oxide release. *Proceedings of the National Academy of Sciences of the United States of America*. 104(41):16281–16286. doi:<https://doi.org/10.1073/pnas.0707791104>. [accessed 2021 May 8]. <https://pubmed.ncbi.nlm.nih.gov/17911245/>.

Olde Engberink RHG, Rorije NMG, Homan van der Heide JJ, van den Born B-JH, Vogt L. 2014. Role of the Vascular Wall in Sodium Homeostasis and Salt Sensitivity. *Journal of the American Society of Nephrology*. 26(4):777–783. doi:<https://doi.org/10.1681/asn.2014050430>.

Olde Engberink RHG, Selvarajah V, Vogt L. 2019. Clinical impact of tissue sodium storage. *Pediatric Nephrology*. 35(8):1373–1380. doi:<https://doi.org/10.1007/s00467-019-04305-8>.

Oohira A, Wight TN, Bornstein P. 1983. Sulfated proteoglycans synthesized by vascular endothelial cells in culture. *Journal of Biological Chemistry*. 258(3):2014–2021. doi:[https://doi.org/10.1016/S0021-9258\(18\)33090-4](https://doi.org/10.1016/S0021-9258(18)33090-4). [accessed 2024 Feb 28]. <https://www.sciencedirect.com/science/article/pii/S0021925818330904?via%3Dihub>.

Pahakis MY, Kosky JR, Dull RO, Tarbell JM. 2007. The role of endothelial glycocalyx components in mechanotransduction of fluid shear stress. *Biochemical and Biophysical Research Communications*. 355(1):228–233. doi:<https://doi.org/10.1016/j.bbrc.2007.01.137>. https://www.sciencedirect.com/science/article/pii/S0006291X07002021?casa_token=PwbLFPJ3ShUAAAAA:0vdjlG9cD0G19VKZzWB-uAKGz7LsO_s7dTGv0vFP9ihZuoinlMU6_0HGL5luocK3AZzPNx_.

Patik JC, Lennon SL, Farquhar WB, Edwards DG. 2021. Mechanisms of Dietary Sodium-Induced Impairments in Endothelial Function and Potential Countermeasures. *Nutrients*. 13(1):270. doi:<https://doi.org/10.3390/nu13010270>.

Paul S, Lal G. 2017. The Molecular Mechanism of Natural Killer Cells Function and Its Importance in Cancer Immunotherapy. *Frontiers in Immunology*. 8(1124). doi:<https://doi.org/10.3389/fimmu.2017.01124>. <https://www.ncbi.nlm.nih.gov/pmc/articles/PMC5601256/>.

Peake JM, Neubauer O, Della Gatta PA, Nosaka K. 2017. Muscle damage and inflammation during recovery from exercise. *Journal of Applied Physiology*. 122(3):559–570.

Peake JM, Neubauer O, Walsh NP, Simpson RJ. 2017. Recovery of the immune system after exercise. *Journal of Applied Physiology*. 122(5):1077–1087. doi:<https://doi.org/10.1152/jappphysiol.00622.2016>.

Petersen AMW, Pedersen BK. 2005. The anti-inflammatory effect of exercise. *Journal of Applied Physiology*. 98(4):1154–1162. doi:<https://doi.org/10.1152/jappphysiol.00164.2004>.

- Philips Healthcare. Epiq 5 Ultrasound System for Vascular. USA: Philips Healthcare; [May 4, 2024]. Available from: <https://www.usa.philips.com/healthcare/product/HC795204V/epiq-5-ultrasound-system-for-vascular>
- Pyke KE, Tschakovsky ME. 2005. The relationship between shear stress and flow-mediated dilatation: implications for the assessment of endothelial function. *The Journal of Physiology*. 568(2):357–369. doi:<https://doi.org/10.1113/jphysiol.2005.089755>.
- Qamirani E, Ren Y, Kuo L, Hein TW. 2005. C-Reactive Protein Inhibits Endothelium-Dependent NO-Mediated Dilation in Coronary Arterioles by Activating p38 Kinase and NAD(P)H Oxidase. *Arteriosclerosis, thrombosis, and vascular biology*. 25(5):995–1001. doi:<https://doi.org/10.1161/01.atv.0000159890.10526.1e>.
- Qian J, Fulton D. 2013. Post-translational regulation of endothelial nitric oxide synthase in vascular endothelium. *Frontiers in Physiology*. 4. doi:<https://doi.org/10.3389/fphys.2013.00347>.
- Qu J, Cheng Y, Wu W, Yuan L, Liu X. 2021. Glycocalyx Impairment in Vascular Disease: Focus on Inflammation. *Frontiers in Cell and Developmental Biology*. 9. doi:<https://doi.org/10.3389/fcell.2021.730621>.
- Quindry JC, Stone WL, King J, Broeder CE. 2003. The Effects of Acute Exercise on Neutrophils and Plasma Oxidative Stress. *Medicine & Science in Sports & Exercise*. 35(7):1139–1145. doi:<https://doi.org/10.1249/01.mss.0000074568.82597.0b>.
- Quintana-Mendias E, Rodríguez-Villalobos JM, Gastelum-Arellanez A, Cervantes N, Carrasco-Legleu CE, Espino-Solis GP. 2023. The Effect of Acute Physical Exercise on Natural Killer Cells Populations and Cytokine Levels in Healthy Women. *Sports*. 11(10):189. doi:<https://doi.org/10.3390/sports11100189>. <https://www.mdpi.com/2075-4663/11/10/189>.
- Reed BG, Carr BR. 2018 Aug 5. The Normal Menstrual Cycle and the Control of Ovulation. Nihgov. <https://www.ncbi.nlm.nih.gov/books/NBK279054/>.
- Reitsma S, Slaaf DW, Vink H, van Zandvoort MAMJ, Olde Egbrink MGA. 2007. The endothelial glycocalyx: composition, functions, and visualization. *Pflügers Archiv - European Journal of Physiology*. 454(3):345–359. doi:<https://doi.org/10.1007/s00424-007-0212-8>. <https://www.ncbi.nlm.nih.gov/pmc/articles/PMC1915585/>.
- Rizvi ZA, Dalal R, Sadhu S, Kumar Y, Kumar S, Gupta SK, Tripathy MR, Rathore DK, Awasthi A. 2021. High-salt diet mediates interplay between NK cells and gut microbiota to induce potent tumor immunity. *Science Advances*. 7(37). doi:<https://doi.org/10.1126/sciadv.abg5016>.
- Rosenberry R, Nelson MD. 2020. Reactive hyperemia: a review of methods, mechanisms, and considerations. *American Journal of Physiology-Regulatory, Integrative and Comparative Physiology*. 318(3):R605–R618. doi:<https://doi.org/10.1152/ajpregu.00339.2019>.
- Rossiter HB. 2011. Exercise: Kinetic considerations for gas exchange. *Comprehensive Physiology*. 1(1):203–44. doi:<https://doi.org/10.1002/cphy.c090010>. <https://www.ncbi.nlm.nih.gov/pubmed/23737170>.

- Rowbottom DG, Green KJ. 2000. Acute exercise effects on the immune system. *Medicine & Science in Sports & Exercise*. 32(7):S396. https://journals.lww.com/acsm-msse/Fulltext/2000/07001/Acute_exercise_effects_on_the_immune_system.4.aspx.
- Sapp RM, Shill DD, Dash C, Hicks JC, Adams-Campbell LL, Hagberg JM. 2019. Circulating microRNAs and endothelial cell migration rate are associated with metabolic syndrome and fitness level in postmenopausal African American women. *Physiological Reports*. 7(14). doi:<https://doi.org/10.14814/phy2.14173>.
- Sakellariou GK, Jackson MJ, Vasilaki A. 2013. Redefining the major contributors to superoxide production in contracting skeletal muscle. The role of NAD(P)H oxidases. *Free Radical Research*. 48(1):12–29. doi:<https://doi.org/10.3109/10715762.2013.830718>.
- Sand KL, Flatebo T, Andersen MB, Maghazachi AA. 2013. Effects of exercise on leukocytosis and blood hemostasis in 800 healthy young females and males. *World Journal of Experimental Medicine*. 3(1):11–20. doi:<https://doi.org/10.5493/wjem.v3.i1.11>. <https://www.ncbi.nlm.nih.gov/pmc/articles/PMC3905589/>.
- Sarelius I, Pohl U. 2010. Control of muscle blood flow during exercise: local factors and integrative mechanisms. *Acta Physiologica*. 199(4):349–365. doi:<https://doi.org/10.1111/j.1748-1716.2010.02129.x>. <https://www.ncbi.nlm.nih.gov/pmc/articles/PMC3157959/>.
- Schmitz B, Niehues H, Lenders M, Thorwesten L, Klose A, Krüger M, Brand E, Brand S-M. 2019. Effects of high-intensity interval training on microvascular glycocalyx and associated microRNAs. *American Journal of Physiology-Heart and Circulatory Physiology*. 316(6):H1538–H1551. doi:<https://doi.org/10.1152/ajpheart.00751.2018>.
- Schlagheck ML, Walzik D, Joisten N, Koliymitra C, Hardt L, Metcalfe AJ, Wahl P, Bloch W, Schenk A, Zimmer P. 2020. Cellular immune response to acute exercise: Comparison of endurance and resistance exercise. *European Journal of Haematology*. 105(1):75–84. doi:<https://doi.org/10.1111/ejh.13412>.
- Sędek Ł, Kulis J, Słota Ł, Twardoch M, Pierzyna-Światała M, Perkowski B, Szczepański T. 2020. The influence of fixation of biological samples on cell count and marker expression stability in flow cytometric analyses. *Central European Journal of Immunology*. 45(2):206–213. doi:<https://doi.org/10.5114/ceji.2020.95858>. <https://www.ncbi.nlm.nih.gov/pmc/articles/PMC7792444/>.
- Selvarajah V, Mäki-Petäjä KM, Pedro L, Bruggraber SFA, Burling K, Goodhart AK, Brown MJ, McEniery CM, Wilkinson IB. 2017. Novel Mechanism for Buffering Dietary Salt in Humans. *Hypertension*. 70(5):930–937. doi:<https://doi.org/10.1161/hypertensionaha.117.10003>.
- Shamloo K, Mistry P, Barbarino A, Ross C, Jhanji V, Sharma A. 2021. Differential Effect of Proinflammatory Cytokines on Corneal and Conjunctival Epithelial Cell Mucins and Glycocalyx. *Translational Vision Science & Technology*. 10(7):17. doi:<https://doi.org/10.1167/tvst.10.7.17>.

Solberg G, Robstad B, Skjønberg OH, Borchsenius F. 2005. Respiratory gas exchange indices for estimating the anaerobic threshold. *Journal of sports science & medicine*. 4(1):29–36. <https://www.ncbi.nlm.nih.gov/pmc/articles/PMC3880081/>.

Sproston NR, Ashworth JJ. 2018. Role of C-Reactive Protein at Sites of Inflammation and Infection. *Frontiers in Immunology*. 9(754). doi:<https://doi.org/10.3389/fimmu.2018.00754>. <https://www.ncbi.nlm.nih.gov/pmc/articles/PMC5908901/>.

Steinach M, Biere K, Coker RH, Gaul AL, Hoerl M, Jörres M, Kienast C, Mascarell-Maricic L, Schalt A, Gunga H-C, et al. 2022. Influences on glycocalyx shedding during the Yukon Arctic Ultra: the longest and the coldest ultramarathon. *Journal of Applied Physiology*. 133(5):1119–1135. doi:<https://doi.org/10.1152/jappphysiol.00180.2022>.

Steinbacher P, Eckl P. 2015. Impact of Oxidative Stress on Exercising Skeletal Muscle. *Biomolecules*. 5(2):356–377. doi:<https://doi.org/10.3390/biom5020356>.

Strazzullo P, D’Elia L, Kandala N-B., Cappuccio FP. 2009. Salt intake, stroke, and cardiovascular disease: meta-analysis of prospective studies. *BMJ*. 339(nov24 1):b4567–b4567. doi:<https://doi.org/10.1136/bmj.b4567>.

Tan BL, Norhaizan ME, Liew W-P-P, Sulaiman Rahman H. 2018. Antioxidant and Oxidative Stress: A Mutual Interplay in Age-Related Diseases. *Frontiers in Pharmacology*. 9(1162). doi:<https://doi.org/10.3389/fphar.2018.01162>.

Tarbell JM, Cancel LM. 2016. The glycocalyx and its significance in human medicine. *Journal of Internal Medicine*. 280(1):97–113. doi:<https://doi.org/10.1111/joim.12465>.

Tarbell JM, Pahakis MY. 2006. Mechanotransduction and the glycocalyx. *Journal of Internal Medicine*. 259(4):339–350. doi:<https://doi.org/10.1111/j.1365-2796.2006.01620.x>.

Tauler P, Aguiló A, Fuentespina E, Tur J, Pons A. 2002. Diet supplementation with vitamin E, vitamin C and β -carotene cocktail enhances basal neutrophil antioxidant enzymes in athletes. *Pflügers Archiv - European Journal of Physiology*. 443(5):791–797. doi:<https://doi.org/10.1007/s00424-001-0770-0>.

Titze J, Shakibaei M, Schafflhuber M, Schulze-Tanzil G, Porst M, Schwind KH, Dietsch P, Hilgers KF. 2004. Glycosaminoglycan polymerization may enable osmotically inactive Na⁺ storage in the skin. *American Journal of Physiology-Heart and Circulatory Physiology*. 287(1):H203–H208. doi:<https://doi.org/10.1152/ajpheart.01237.2003>.

Tran N, Garcia T, Aniqá M, Ali S, Ally A, Nauli SM. 2022. Endothelial Nitric Oxide Synthase (eNOS) and the Cardiovascular System: in Physiology and in Disease States. *American journal of biomedical science & research*. 15(2):153. [accessed 2024 Jan 9]. <https://www.ncbi.nlm.nih.gov/pmc/articles/PMC8774925/#:~:text=It%20is%20now%20known%20how>.

Tvede N, Kappel M, Halkjær-Kristensen J, Galbo H, Pedersen B. 1993. The Effect of Light, Moderate and Severe Bicycle Exercise on Lymphocyte Subsets, Natural and Lymphokine

Activated Killer Cells, Lymphocyte Proliferative Response and Interleukin 2 Production. *International Journal of Sports Medicine*. 14(05):275–282. doi:<https://doi.org/10.1055/s-2007-1021177>.

Ueda H, Tsuchiya Y, Ochi E. 2020. Fast-Velocity Eccentric Cycling Exercise Causes Greater Muscle Damage Than Slow Eccentric Cycling. *Frontiers in Physiology*. 11. doi:<https://doi.org/10.3389/fphys.2020.596640>.

Vivier E, Tomasello E, Baratin M, Walzer T, Ugolini S. 2008. Functions of natural killer cells. *Nature Immunology*. 9(5):503–510. doi:<https://doi.org/10.1038/ni1582>.

Volpi N. 1999. Disaccharide Analysis and Molecular Mass Determination to Microgram Level of Single Sulfated Glycosaminoglycan Species in Mixtures Following Agarose-Gel Electrophoresis. *Analytical Biochemistry*. 273(2):229–239. doi:<https://doi.org/10.1006/abio.1999.4218>.

Wander K, Brindle E, O'Connor KA. 2008. C-reactive protein across the menstrual cycle. *American Journal of Physical Anthropology*. 136(2):138–146. doi:<https://doi.org/10.1002/ajpa.20785>.

Wang Y-J, Yeh T-L, Shih M-C, Tu Y-K, Chien K-L. 2020. Dietary Sodium Intake and Risk of Cardiovascular Disease: A Systematic Review and Dose-Response Meta-Analysis. *Nutrients*. 12(10):2934. doi:<https://doi.org/10.3390/nu12102934>.
<https://www.ncbi.nlm.nih.gov/pmc/articles/PMC7601012/>.

Weinbaum S, Tarbell JM, Damiano ER. 2007. The structure and function of the endothelial glycocalyx layer. *Annual Review of Biomedical Engineering*. 9:121–167. doi:<https://doi.org/10.1146/annurev.bioeng.9.060906.151959>.
<https://pubmed.ncbi.nlm.nih.gov/17373886/>.

Weinbaum S, Zhang X-B, Han Y, Vink H, Cowin SC. 2003. Mechanotransduction and flow across the endothelial glycocalyx. *Proceedings of the National Academy of Sciences of the United States of America*. 100(13):7988–7995. doi:<https://doi.org/10.1073/pnas.1332808100>.

Wenstedt EFE, Oppelaar JJ, Besseling S, Roije NMG, Olde Engberink RHG, Oosterhof A, Kuppevelt TH, van den Born B-JH, Aten J, Vogt L. 2021. Distinct osmoregulatory responses to sodium loading in patients with altered glycosaminoglycan structure: a randomized cross-over trial. *Journal of translational medicine*. 19(1). doi:<https://doi.org/10.1186/s12967-021-02700-0>. [accessed 2024 Apr 27]. <https://www.ncbi.nlm.nih.gov/pmc/articles/PMC7816310/>.

Wenstedt EFE, Verberk SGS, Kroon J, Neele AE, Baardman J, Claessen N, Pasaoglu ÖT, Rademaker E, Schrooten EM, Wouda RD, et al. 2019. Salt increases monocyte CCR2 expression and inflammatory responses in humans. *JCI insight*. 4(21). doi:<https://doi.org/10.1172/jci.insight.130508>. [accessed 2024 May 1]. <https://www.ncbi.nlm.nih.gov/pmc/articles/PMC6948772/>.

Wonner R, Wallner S, Orsó E, Schmitz G. 2016. Effects of acute exercise on monocyte subpopulations in metabolic syndrome patients. *Cytometry Part B: Clinical Cytometry*. 94(4):596–605. doi:<https://doi.org/10.1002/cyto.b.21387>.

World Health Organization. 2023 Mar 9. WHO global report on sodium intake reduction. [www.who.int. https://www.who.int/publications/i/item/9789240069985](http://www.who.int/publications/i/item/9789240069985).

Yi B, Titze J, Rykova M, Feuerecker M, Vassilieva G, Nichiporuk I, Schelling G, Morukov B, Choukèr A. 2015. Effects of dietary salt levels on monocytic cells and immune responses in healthy human subjects: a longitudinal study. *Translational Research: The Journal of Laboratory and Clinical Medicine*. 166(1):103–110. doi:<https://doi.org/10.1016/j.trsl.2014.11.007>. [accessed 2020 Nov 8]. <https://pubmed.ncbi.nlm.nih.gov/25497276/>.

Younus H. 2018. Therapeutic potentials of superoxide dismutase. *International journal of health sciences*. 12(3):88–93. <https://www.ncbi.nlm.nih.gov/pmc/articles/PMC5969776/#:~:text=SODs%20form%20the%20front%20line>.

Zahnd G, Orkisz M, Vray D. 2017. CAROLAB, doi:10.5281/zenodo.398680

Zeng X, Li Y, Lv W, Dong X, Zeng C, Zeng L, Wei Z, Lin X, Ma Y, Xiao Q. 2020. A High-Salt Diet Disturbs the Development and Function of Natural Killer Cells in Mice. *Journal of Immunology Research*. 2020:1–15. doi:<https://doi.org/10.1155/2020/6687143>. [accessed 2021 Nov 2]. <https://eds.p.ebscohost.com/eds/pdfviewer/pdfviewer?vid=1&sid=eff3e62d-3d53-4bd4-967d-dbf3c332cf3b%40redis>.

Zhang W-C, Zheng X-J, Du L-J, Sun J-Y, Shen Z-X, Shi C, Sun S, Zhang Z, Chen X, Qin M, et al. 2015. High salt primes a specific activation state of macrophages, M(Na). *Cell Research*. 25(8):893–910. doi:<https://doi.org/10.1038/cr.2015.87>.

Zhu J, Huang T, Lombard JH. 2007. Effect of High-Salt Diet on Vascular Relaxation and Oxidative Stress in Mesenteric Resistance Arteries. *Journal of Vascular Research*. 44(5):382–390. doi:<https://doi.org/10.1159/000102955>.

Zuo L, Zhou T, Pannell BK, Ziegler AC, Best TM. 2015. Biological and physiological role of reactive oxygen species - the good, the bad and the ugly. *Acta Physiologica*. 214(3):329–348. doi:<https://doi.org/10.1111/apha.12515>.

APPENDICES

Appendix 1

Statistical analysis

Statistics from 3-way RM ANOVA performed on popliteal FMD data across conditions of exercise (pre and post), time (before and after), and condition (salt and control) (n=4).

Within Subjects Effects

Cases	Sum of Squares	df	Mean Square	F	p
condition	2.239	1	2.239	0.602	0.494
Residuals	11.163	3	3.721		
time	0.017	1	0.017	0.004	0.956
Residuals	14.470	3	4.823		
exercise	56.352	1	56.352	99.274	0.002
Residuals	1.703	3	0.568		
condition * time	2.576	1	2.576	1.240	0.347
Residuals	6.234	3	2.078		
condition * exercise	6.706	1	6.706	1.080	0.375
Residuals	18.620	3	6.207		
time * exercise	0.864	1	0.864	0.061	0.821
Residuals	42.555	3	14.185		
condition * time * exercise	1.960	1	1.960	0.521	0.523
Residuals	11.285	3	3.762		

Note. *Type III Sum of Squares.*

Statistics from 3-way RM ANOVA performed on brachial FMD data across exercise (pre and post), time (before and after), and condition (salt and control) (n=4).

Within Subjects Effects

Cases	Sum of Squares	df	Mean Square	F	p
condition	4.435	1	4.435	0.691	0.467
Residuals	19.250	3	6.417		
time	1.946	1	1.946	0.100	0.772
Residuals	58.332	3	19.444		
exercise	1.086	1	1.086	0.406	0.570
Residuals	8.037	3	2.679		
condition * time	2.450	1	2.450	0.530	0.519
Residuals	13.864	3	4.621		
condition * exercise	2.003	1	2.003	1.645	0.290
Residuals	3.653	3	1.218		
time * exercise	0.320	1	0.320	0.112	0.760
Residuals	8.539	3	2.846		
condition * time * exercise	0.015	1	0.015	0.002	0.966
Residuals	20.574	3	6.858		

Note. Type III Sum of Squares.

Statistics from 3-way repeated measures ANOVA analysis of leukocyte cells/ μl across exercise (pre and post), time (before and after), and condition (salt and control) (n=4).

Within Subjects Effects

Cases	Sum of Squares	df	Mean Square	F	p
condition	437776.602	1	437776.602	0.774	0.444
Residuals	$1.696 \times 10^{+6}$	3	565382.652		
time	519720.710	1	519720.710	0.550	0.512
Residuals	$2.836 \times 10^{+6}$	3	945210.275		
exercise	63829.859	1	63829.859	0.052	0.835
Residuals	$3.701 \times 10^{+6}$	3	$1.234 \times 10^{+6}$		
condition * time	857.601	1	857.601	0.001	0.975
Residuals	$2.228 \times 10^{+6}$	3	742583.456		
condition * exercise	63710.221	1	63710.221	1.028	0.385
Residuals	185996.068	3	61998.689		
time * exercise	607301.184	1	607301.184	0.806	0.436
Residuals	$2.261 \times 10^{+6}$	3	753710.499		
condition * time * exercise	1812.923	1	1812.923	0.052	0.835
Residuals	105211.173	3	35070.391		

Note. Type III Sum of Squares.

Statistics from 3-way repeated measures ANOVA analysis of neutrophil cells/ μ l across exercise (pre and post), time (before and after), and condition (salt and control) (n=4).

Within Subjects Effects

Cases	Sum of Squares	df	Mean Square	F	p
condition	192750.644	1	192750.644	0.674	0.472
Residuals	858145.877	3	286048.626		
time	82423.075	1	82423.075	0.101	0.772
Residuals	2.455 $\times 10^{+6}$	3	818435.277		
exercise	36234.993	1	36234.993	0.041	0.852
Residuals	2.633 $\times 10^{+6}$	3	877788.859		
condition * time	5164.583	1	5164.583	0.012	0.918
Residuals	1.246 $\times 10^{+6}$	3	415205.699		
condition * exercise	75220.599	1	75220.599	1.493	0.309
Residuals	151177.490	3	50392.497		
time * exercise	772844.606	1	772844.606	1.991	0.253
Residuals	1.165 $\times 10^{+6}$	3	388226.868		
condition * time * exercise	2007.086	1	2007.086	0.032	0.869
Residuals	185771.068	3	61923.689		

Note. Type III Sum of Squares

Statistics from 3-way repeated measures ANOVA analysis of monocyte cells/ μl across exercise (pre and post), time (before and after), and condition (salt and control) (n=4).

Within Subjects Effects

Cases	Sum of Squares	df	Mean Square	F	p
condition	768.026	1	768.026	0.328	0.607
Residuals	7019.634	3	2339.878		
time	3256.043	1	3256.043	12.911	0.037*
Residuals	756.585	3	252.195		
exercise	168.040	1	168.040	0.055	0.830
Residuals	9180.379	3	3060.126		
condition * time	2448.075	1	2448.075	1.367	0.327
Residuals	5374.058	3	1791.353		
condition * exercise	32.542	1	32.542	0.096	0.777
Residuals	1017.406	3	339.135		
time * exercise	3.207	1	3.207	0.002	0.968
Residuals	5202.066	3	1734.022		
condition * time * exercise	317.709	1	317.709	1.882	0.264
Residuals	506.334	3	168.778		

Note. Type III Sum of Squares. (*) denotes statistically significant change in monocytes per μl .

Statistics from 3-way repeated measures ANOVA analysis of NK cells/ μ l across exercise (pre and post), time (before and after), and condition (salt and control) (n=4).

Within Subjects Effects

Cases	Sum of Squares	df	Mean Square	F	p
condition	513.441	1	513.441	0.304	0.620
Residuals	5063.633	3	1687.878		
time	12200.001	1	12200.001	0.874	0.419
Residuals	41855.398	3	13951.799		
exercise	73.872	1	73.872	0.038	0.859
Residuals	5901.641	3	1967.214		
condition * time	827.228	1	827.228	0.544	0.514
Residuals	4561.885	3	1520.628		
condition * exercise	0.702	1	0.702	0.001	0.973
Residuals	1591.815	3	530.605		
times * exercise	2313.700	1	2313.700	1.550	0.302
Residuals	4477.824	3	1492.608		
condition * time * exercise	36.509	1	36.509	0.079	0.797
Residuals	1390.703	3	463.568		

Note. Type III Sum of Squares.

Statistics from 3-way repeated measures ANOVA analysis of neutrophil proportion of the total leukocyte population for, condition (salt or sugar), time (before or after), and exercise (pre- and post-exercise) measured through flow cytometry (n=4).

Within Subjects Effects

Cases	Sum of Squares	df	Mean Square	F	p
condition	0.005	1	0.005	0.702	0.464
Residuals	0.020	3	0.007		
time	1.205×10 ⁻⁴	1	1.205×10 ⁻⁴	0.012	0.920
Residuals	0.030	3	0.010		
exercise	0.002	1	0.002	0.345	0.598
Residuals	0.021	3	0.007		
condition * time	0.006	1	0.006	0.731	0.455
Residuals	0.023	3	0.008		
condition * exercise	1.431×10 ⁻⁴	1	1.431×10 ⁻⁴	0.107	0.765
Residuals	0.004	3	0.001		
time * exercise	0.008	1	0.008	3.328	0.166
Residuals	0.007	3	0.002		
condition * time * exercise	2.022×10 ⁻⁴	1	2.022×10 ⁻⁴	0.083	0.792
Residuals	0.007	3	0.002		

Note. Type III Sum of Squares.

Statistics from 3-way repeated measures ANOVA analysis of monocyte proportion of the total leukocyte population for, condition (salt or sugar), time (before or after), and exercise (pre- and post-exercise) measured through flow cytometry (n=4).

Within Subjects Effects

Cases	Sum of Squares	df	Mean Square	F	p
condition	1.476×10 ⁻⁴	1	1.476×10 ⁻⁴	0.983	0.394
Residuals	4.503×10 ⁻⁴	3	1.501×10 ⁻⁴		
time	1.003×10 ⁻⁵	1	1.003×10 ⁻⁵	0.038	0.858
Residuals	7.937×10 ⁻⁴	3	2.646×10 ⁻⁴		
exercise	1.575×10 ⁻⁴	1	1.575×10 ⁻⁴	1.192	0.355
Residuals	3.965×10 ⁻⁴	3	1.322×10 ⁻⁴		
condition * time	2.632×10 ⁻⁴	1	2.632×10 ⁻⁴	2.425	0.217
Residuals	3.256×10 ⁻⁴	3	1.085×10 ⁻⁴		
condition * time	2.661×10 ⁻⁶	1	2.661×10 ⁻⁶	0.080	0.795
Residuals	9.938×10 ⁻⁵	3	3.313×10 ⁻⁵		
time * exercise	5.036×10 ⁻⁵	1	5.036×10 ⁻⁵	0.917	0.409
Residuals	1.647×10 ⁻⁴	3	5.491×10 ⁻⁵		
condition * time * exercise	2.180×10 ⁻⁶	1	2.180×10 ⁻⁶	0.088	0.787
Residuals	7.462×10 ⁻⁵	3	2.487×10 ⁻⁵		

Note. Type III Sum of Squares.

Statistics from 3-way repeated measures ANOVA analysis of NK cell proportion of the total leukocyte population for, condition (salt or sugar), time (before or after), and exercise (pre- and post-exercise) measured through flow cytometry (n=4).

Within Subjects Effects

Cases	Sum of Squares	df	Mean Square	F	p
condition	4.262×10 ⁻⁵	1	4.262×10 ⁻⁵	0.203	0.683
Residuals	6.297×10 ⁻⁴	3	2.099×10 ⁻⁴		
time	3.500×10 ⁻⁴	1	3.500×10 ⁻⁴	0.702	0.464
Residuals	0.001	3	4.986×10 ⁻⁴		
exercise	2.182×10 ⁻⁴	1	2.182×10 ⁻⁴	0.485	0.536
Residuals	0.001	3	4.500×10 ⁻⁴		
condition * time	4.324×10 ⁻⁵	1	4.324×10 ⁻⁵	0.207	0.680
Residuals	6.268×10 ⁻⁴	3	2.089×10 ⁻⁴		
condition * time	4.130×10 ⁻⁶	1	4.130×10 ⁻⁶	0.039	0.857
Residuals	3.212×10 ⁻⁴	3	1.071×10 ⁻⁴		
time * exercise	2.574×10 ⁻⁴	1	2.574×10 ⁻⁴	1.363	0.327
Residuals	5.666×10 ⁻⁴	3	1.889×10 ⁻⁴		
treatment * time * exercise	4.186×10 ⁻⁶	1	4.186×10 ⁻⁶	0.039	0.856
Residuals	3.218×10 ⁻⁴	3	1.073×10 ⁻⁴		

Note. Type III Sum of Squares.

Abbreviations

Abbreviation	Definition
Na ⁺	Sodium
CVD	Cardiovascular Disease
BP	Blood Pressure
ESL	Endothelial Surface Layer
GAG	Glycosaminoglycan
NO	Nitric Oxide
HS	Heparan Sulfate
HA	Hyaluronic Acid
eGC	Endothelial Glycocalyx
eNOS	Endothelial Nitric Oxide Synthase
BH ₄	Tetrahydrobiopterin
NADPH	Nicotinamide Adenine Dinucleotide Phosphate
FAD	Flavin Adenine Dinucleotide
FMN	Flavin Mononucleotide
sGC	Guanylyl Cyclase
cGMP	Cyclic Guanosine Monophosphate
GTP	Guanosine Triphosphate
GPCR	G-protein Coupled Receptors
PLC	Phospholipase C
DAG	Diacylglycerol
IP ₃	Inositol 1,4,5-trisphosphate
MLCK	Myosin Light Chain Kinase
MLCP	Myosin Light Chain Phosphatase
ROS	Reactive Oxygen Species
O ₂ ⁻	Superoxide
ONOO ⁻	Peroxynitrite
SOD	Superoxide Dismutase
FMD	Flow-mediated Dilation
H ₂ O ₂	Hydrogen Peroxide
ENaC	epithelial Na ⁺ Channels
SDC-1	Syndecan-1
LPS	Lipopolysaccharide
TNF- α	Tumour Necrosis Factor Alpha
IL-1 β	Interleukin-1 Beta
IL-6	Interleukin-6
CCR2	C-C Chemokine Receptor Type 2
MCP-1	Monocyte Chemoattractant Protein-1

VEGF-C	Vascular Endothelial Growth Factor-C
NK cells	Natural Killer Cells
PAR-Q+	Physical Activity Readiness +
RQ	Respiratory Quotient
VT1	Ventilatory Threshold 1
CO ₂	Carbon Dioxide
VO ₂	Oxygen Uptake
VCO ₂	Carbon Dioxide Output
VE	Minute Ventilation
VT2	Ventilatory Threshold 2
ECG	Electrocardiogram
ELISA	Enzyme-linked Immunosorbent Assay
PPG	Photoplethysmography
CNAP	Continuous Non-invasive Arterial Pressure Monitoring
HR	Heart Rate
CRP	C-reactive Protein
IL-1ra	Interleukin-1 Receptor Antagonist
IL-10	Interleukin-10
CK	Creatine Kinase
HOCl	Hypochlorous Acid
MPO	Myeloperoxidase
IFN- γ	Interferon- γ
IL-1	Interleukin-1
TNF	Tumour Necrosis Factor
GM-CSF	Granulocyte-Macrophage Colony-Stimulating Factor